Critical Reviews in Oncology / Hematology 169 (2022) 103544

Contents lists available at ScienceDirect

Critical Reviews in Oncology / Hematology

journal homepage: www.elsevier.com/locate/critrevonc

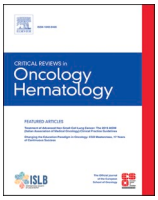

State of the art of radiomic analysis in the clinical management of prostate cancer: A systematic review

Samuele Ghezzo [a], Carolina Bezzi [a], Luca Presotto [b], Paola Mapelli [a,b], Valentino Bettinardi [b], Annarita Savi [b], Ilaria Neri [b], Erik Preza [b], Ana Maria Samanes Gajate [b], Francesco De Cobelli [a,c], Paola Scifo [b], Maria Picchio [a,b,*]

[a] Vita-Salute San Raffaele University, Milan, Italy
[b] Nuclear Medicine Department, IRCCS San Raffaele Scientific Institute, Milan, Italy
[c] Radiology Department, IRCCS San Raffaele Scientific Institute, Milan, Italy

ARTICLE INFO

Keywords:
Radiomics
Prostate cancer
MRI
PET
CT
Clinical management

ABSTRACT

We present the current clinical applications of radiomics in the context of prostate cancer (PCa) management. Several online databases for original articles using a combination of the following keywords: "(radiomic or radiomics) AND (prostate cancer or prostate tumour or prostate tumor or prostate neoplasia)" have been searched. The selected papers have been pooled as focus on (i) PCa detection, (ii) assessing the clinical significance of PCa, (iii) biochemical recurrence prediction, (iv) radiation-therapy outcome prediction and treatment efficacy monitoring, (v) metastases detection, (vi) metastases prediction, (vii) prediction of extra-prostatic extension. Seventy-six studies were included for qualitative analyses. Classifiers powered with radiomic features were able to discriminate between healthy tissue and PCa and between low- and high-risk PCa. However, before radiomics can be proposed for clinical use its methods have to be standardized, and these first encouraging results need to be robustly replicated in large and independent cohorts.

1. Introduction

Prostate cancer (PCa) affects over four million individuals and is the second most common cancer in men worldwide (World Health Organization, 2020). Early diagnosis is a key contributor to successful PCa management, with remarkable consequences on its relatively low mortality rate. Digital rectal examination (DRE), trans-rectal ultrasound (TRUS), and prostate-specific antigen (PSA) serum level are commonly used for PCa screening (Schröder et al., 2009). However, although sensitive, these tests are non-specific, and often result in unnecessary and expensive follow-up procedures (Schröder et al., 2009). Albeit biopsy is currently the gold standard for PCa diagnosis (European Association of Urology, 2020), it has some drawbacks including sampling error, the possibility to cause patients' discomfort and pain and being not representative of the whole tumour heterogeneity (Guo et al., 2018; Kristiansen, 2012; Patel et al., 2014; Marusyk and Polyak, 2010).

Multi-parametric Magnetic Resonance Imaging (mp-MRI) has the potential to reliably detect PCa, reducing the number of unnecessary biopsies by guiding a more precise sampling (Carlaw and Woo, 2017; Gupta et al., 2013). The prostate imaging-reporting and data systems (PI-RADS) version 2 was released in 2015 for the standardization of the interpretation of mp-MRI scans (American College of Radiology Web site, 2015). Since its introduction it has reached widespread acceptance and it is now regularly implemented in patient care (Kasel-Seibert et al., 2016), where it has improved diagnostic accuracy of PCa up to 60–90 % (Jordan et al., 2017). However, PI-RADS v2 features are subjective and therefore susceptible to inter- and intra-observer variability (Rosenkrantz et al., 2016).

Radiomics has been defined as "high throughput extraction of quantitative features that results in the conversion of images into mineable data" (Gillies et al., 2016). More simply, radiomics consists in the extraction of quantitative information from medical images. This method uses features based on intensity, shape, size, volume, and texture to accurately describe the tumour phenotype. Radiomics potentially provides several quantitative, objective, imaging biomarkers that can aid in personalized PCa management (Gillies et al., 2016; Yip and Aerts, 2016). Another advantage of radiomics is that it makes use of different kinds of imaging modalities, raising the possibility to

* Corresponding author at: Nuclear Medicine Department, IRCCS San Raffaele Scientific Institute, Via Olgettina 60, 20132, Milan, Italy.
E-mail address: picchio.maria@hsr.it (M. Picchio).

https://doi.org/10.1016/j.critrevonc.2021.103544
Received 28 July 2021; Received in revised form 18 October 2021; Accepted 18 October 2021
Available online 18 November 2021

investigate multiple aspects of the tumour at the same time. Furthermore, as information is gathered from the entire tumour mass, this technique offers details on intra-tumoral heterogeneity, which is known to be closely related to cancer progression and therapeutic resistance (Marusyk and Polyak, 2010; Andor et al., 2016).

The field of radiomics is growing fast, yielding promising results, especially in oncology. The rapid progress of radiomics is mainly due to the ever increasing number of medical images that are collected every day and to the advances of machine learning (ML) and deep learning (DL) for their interpretation (Herrmann et al., 2019). The aim of the present review is to systematically report all the applications of radiomics to the clinical management of PCa, discussing the additional utility bore by radiomic analysis to PCa care. Methodological and practical challenges that still prevent radiomics to be applied in clinical settings as well as the adherence to existing guidelines of the included studies will also be discussed.

2. Materials and methods

The following online medical databases have been systematically searched in order to find publications of interest: PubMed, EMBASE, SCOPUS, MEDLINE, and Web of Science using these keywords: (radiomic or radiomics) AND (prostate cancer or prostate tumour or prostate tumor or prostate neoplasia). All publication until December 2020 have been included. After duplicates removal, abstracts were screened to identify and remove all the studies that did not meet the inclusion criteria. The PRISMA diagram showing the detailed selection process, including exclusion criteria, is reported in Fig. 1. Finally, the identified studies were focused on (i) PCa detection, (ii) assessing the clinical significance of PCa, (iii) biochemical recurrence (BCR) prediction, (iv) radiation-therapy (RT) outcome prediction and treatment efficacy monitoring, (v) metastases detection, (vi) metastases prediction, (vii) prediction of extra-prostatic extension (EPE). For each of the included studies the radiomics quality score (RQS) (Lambin et al., 2017) was calculated.

3. Results

3.1. Study selection

Studies were evaluated according to the exclusion/inclusion criteria and 76/571 were finally selected and included for qualitative analysis. The main focus of the selected works is reported in Table 1.

3.2. Prostate cancer detection

Histological examination is required for PCa diagnosis, but selecting good candidates for biopsy is problematic due to the high false-positive rate of screening methods (Schröder et al., 2009). However, mp-MRI have been proved effective in localizing PCa and is now commonly used in clinical practice. The qualitative evaluation of medical images resulted in an increased diagnostic accuracy up to 60–90 %, but it is subject to inter- and intra-observer variability. Radiomics provides the opportunity to evaluate medical images quantitatively and objectively,

Table 1
Studies considered for qualitative analysis.

Topic	Number of studies
Prostate cancer detection	23
Assessing clinical significance of prostate cancer	26
Biochemical recurrence prediction	9
Radiation therapy outcome prediction and treatment efficacy monitoring	9
Metastases detection	6
Metastases prediction	3
Prediction of extra-prostatic extension	4

Note: the same study may be reported in multiple paragraphs.

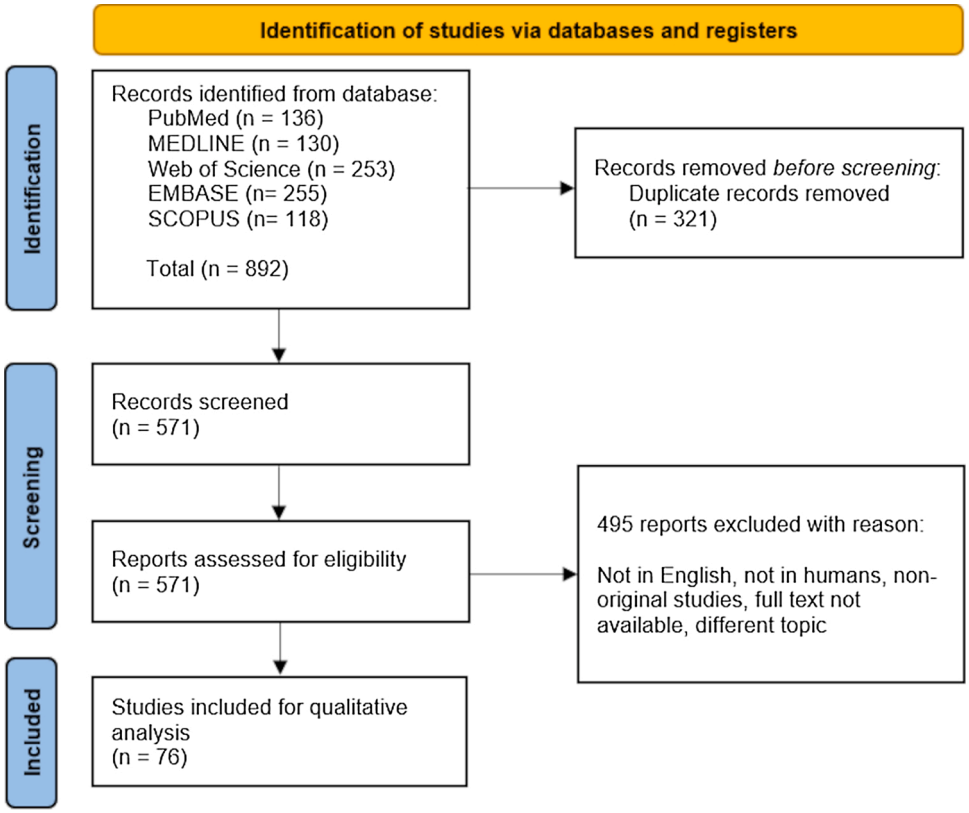

Fig. 1. PRISMA diagram depicting the study selection process.

aiding clinicians in the localization of PCa, thus reducing the amount of unnecessary follow-up procedures.

Classifiers based on mp-MRI radiomic features (RF) have been proved effective in discriminating between healthy and cancerous prostatic tissue (see Table 2). At present, two main approaches were used to automatically localize PCa using radiomics. In the first one, highly sensitive but non-specific algorithms are used to identify potential tumour candidate regions, from which RF are extracted and fed to classifiers that accurately label tumour voxels (Cameron et al., 2016; Khalvati et al., 2018; Chung et al., 2015). Alternatively, supervised (machine) learning (SL) algorithms, trained on a set of labelled images, are reported to precisely classify new, unseen, datasets, reaching area under the operating curve (AUC) > 0.9 for the detection of PCa (Gholizadeh et al., 2020; Khalvati et al., 2015; Zamboglou et al., 2020; Shiradkar et al., 2016; Monti et al., 2020; Wang et al., 2017; Dulhanty et al., 2020; Chen et al., 2019; Qi et al., 2020; Li et al., 2020a; Xu et al., 2019).

Although these results are highly encouraging, and the mean RQS of these studies is 10.87, there are methodological issues hampering the success of radiomic analysis for PCa detection. Only five (Shiradkar et al., 2016; Chen et al., 2019; Qi et al., 2020; Li et al., 2020a; Bagher-Ebadian et al., 2019) out of thirteen studies addressing this topic validated their results in external cohorts, therefore providing an unbiased estimate of the model performance. Furthermore, the majority of the afore presented studies is based on small cohorts (N < 100), only one (Cameron et al., 2016) was prospective and just three (Cameron et al., 2016; Chung et al., 2015; Khalvati et al., 2015) used the histopathological sample collected after surgery as reference standard to define the tumoral area.

Radiomics has been proposed just recently, and therefore, as all young disciplines lacks standardization. It is not clear at present whether DL or ML classifiers are most suited to detect PCa from radiological images, nor which MR sequences store the most relevant information to perform this task. Monti and colleagues (Monti et al., 2020), in a model never validated in separate cohorts, compared the performance of classifiers based on RF extracted from classic imaging modalities like T2 weighted (T2-w) and apparent diffusion coefficient (ADC) with the one of models using RF obtained from more advanced techniques such as diffusion kurtosis imaging (DKI) and dynamic contrast enhanced (DCE). They found that all classifiers were highly precise, with AUC > 0.98 for the discrimination of PCa from healthy tissue (HT). These results led them to conclude that "the inclusion of RF derived from DCE and DKI models does not provide a clear added value for PCa detection", and therefore can be reasonably avoided.

Comparing the performance of radiomic analysis with that of clinical nomograms is necessary to assess the additional utility bore by radiomics for PCa screening. Nevertheless, only five studies (Wang et al., 2017; Dulhanty et al., 2020; Chen et al., 2019; Qi et al., 2020; Li et al., 2020a), of which just two (Chen et al., 2019; Li et al., 2020a) validated in separate sets, examined their results opposed to classifications routinely performed in clinical practice. Here, radiomics was shown to overperform both PI-RADS score (Chen et al., 2019) and a combination of age, PSA density, total PSA, free PSA, and prostate volume (Li et al., 2020a).

Despite the paucity of evidence, it seems that comprehensive models combining RF and clinical data, as done only by (Qi et al. (2020)) and (Li et al. (2020a)), result in the highest accuracy for PCa detection, yielding AUC > 0.9 in validation sets. Therefore, an increased effort to exploit all the available information, not relying on conventional imaging, nor on radiomics or circulating biomarkers only is needed to improve the screening prior to biopsy.

While PI-RADS levels 4 and 5 are strongly associated with clinically significant (cs) PCa, and PI-RADS 1 and 2 are generally indicators of the absence of PCa, PI-RADS 3 lesions are problematic. Lesions classified as PI-RADS 3 are of clinical importance, 20 % estimated being cs after histopathological examination (Hansen et al., 2017; Hou et al., 2020), but are difficult to interpret. Furthermore, at present there is not a consolidated approach to efficiently stratify PI-RADS 3 patients for follow-up procedures. Radiomics could aid clinicians in the identification of csPCa in PI-RADS 3 lesions, allowing adequate treatment planning and improving prognosis.

Giambelluca et al. were the first to perform a discriminant analysis that classified histologically confirmed cs PI-RADS 3 lesions with an accuracy of 80 % (Giambelluca et al., 2021). Although this pioneering work came with several limitations, as it was performed on a small sample (N = 43) without a validation cohort, its results were largely replicated by Hou et al. in 2020 (Hou et al., 2020). In this recent study, T2W, ADC, and DWI based RF were used to train a support vector machine (SVM) providing AUC = 0.89 in the validation set; hence, outperforming two expert physicians in the discrimination between cs and non-significant PI-RADS 3 lesions.

Early disease stages, when qualitative assessment of medical images is more complicated, could also strongly benefit from radiomics. In 2018, Algohary and colleagues (Algohary et al., 2018) in a monocentric retrospective study, stratified 56 patients on active surveillance as having or not csPCa using radiomics, thus reducing the number of false negatives and false positives respectively by 80 and 60 % compared to the evaluation based on PI-RADS scores, potentially avoiding unnecessary follow-up procedures and also reducing the risk of under-treatment.

Whereas the utility of mp-MRI RF for the differential diagnosis of PCa has been largely investigated, only Wildeboer (Wildeboer et al., 2020) retrospectively evaluated the potential of ultrasound (US) RF for the same issue(Wildeboer et al., 2020). In their research they combined B-mode US, shear wave elastography (SWE)-US, and DCE-US RF as input to a random forest classifier validated with the leave-one-patient-out approach, that distinguished HT and PCa with AUC = 0.75.

Conventional imaging provides semi- and quantitative biomarkers for PCa. Domachevsky (Domachevsky et al., 2018) showed that low ADC minimum and mean values, as well as high PET standardized uptake value (SUV) $_{max}$, are indicators of PCa. Similarly, RF also represent objective, quantitative biomarkers for PCa. Zamboglou (Zamboglou et al., 2019) in 2019 reported that 81 % of ^{68}Ga-PSMA PET based RF differ in PCa as compared to HT. Analogously, tumour heterogeneity can be described by RF, specifically by the entropy score (ES) that is measured in natural units of information (NAT). Orczyk and colleagues (Orczyk et al., 2019) calculated the ES from MRI scans and found that this value is higher in PCa than in HT. Localizing PCa by visual assessment or by setting a threshold of 16.61 NAT in ES does not change the performance of the classification (AUC: 0.91 and 0.89, p = 0.75), but using radiomics the positive predicted value (PPV) increases from 24 % to 53 % without hampering the negative predicted value that remains 100 %, thus avoiding unnecessary biopsy in 29 % of cases. Of note, it has to be highlighted that this work lacks proper validation and was based on twenty patients retrospectively enrolled. Further studies, with larger sample size and validation cohorts are required to assess the utility of ES obtained from MRI.

Finally, another aspect to be considered when reading of RF based classifiers for the detection of PCa is that the prostate is subdivided into anatomical zones, and that RF associated with PCa in a specific zone are not necessarily good descriptors of PCa in another one. This was clearly shown by Ginsburg and colleagues (Ginsburg et al., 2017), that found that only half of the top 10 RF for detecting transition zone and peripheral zone tumours are shared across areas.

3.3. Assessing clinical significance

Low grade PCa are suitable candidates for conservative approaches, such as active surveillance, while patients with a more aggressive disease are usually referred to radical interventions like radical prostatectomy (RP) and radiation therapy (RT). To date, biopsy is the golden standard to assess the clinical relevance of PCa, being affected by

Table 2
Radiomics for PCa detection.

Name, year	Data	Clinical setting	Imaging	Radiomic features	Analysis	Outcome	Ground truth	Competitive model	AUC training cohort	AUC validation cohort	RQS
(Cameron et al., 2016)	N = 13, single-centre	Prospective cohort. Patients scheduled for radical prostatectomy, GS ≥ 7	- MRI - Sequences: T2-w, ADC, DWI, CDI	- Extracted: 42 features (morphology, asymmetry, physiology, size) from the whole prostate - Selection method: NO	- Classifier: naïve Bayes classifiers - Validation cohort: NO (leave-one-patient-out validation)	Voxel-wise detection of PCa	Histopathological sample collected after surgery	NA	- Radiomic model: mp-MRI: 0.86	NA	1/36
(Khalvati et al., 2018)	N = 30, single-centre	Retrospective cohort. 17 PCa patients PIRADS ≥ 3, 13 non-PCa patients PIRADS = 2	- MRI - Sequences: T2-w, DWI, ADC, CDI	- Extracted: 96 features (*texture, higher order statistic*) from the whole prostate - Selection method: NO	- Classifier: conditional random field - Validation cohort: NO (leave-one-patient-out validation)	Voxel-wise detection of PCa	Experts' annotation on MRI images using biopsy location on pathology	NA	- Radiomic model: mp-MRI: 0.85	NA	9/36
(Chung et al., 2015)	N = 20, single-centre	Setting not better specified. Patients scheduled for radical prostatectomy, GS ≥ 7	- MRI - Sequences: T2-w, ADC, DWI, CDI	- Extracted: 768 features (*first order statistic, texture, higher order statistic*) from the whole prostate - Selection method: NO	- Classifier: support vector machine + conditional random fields - Validation cohort: NO (leave-one-patient-out validation)	Voxel-wise detection of PCa	Histopathological sample collected after surgery	NA	- Radiomic model: mp-MRI: 0.92	NA	3/36
(Khalvati et al., 2015)	N = 20, single-centre	Retrospective cohort. 17 PCa patients, 3 non-PCa patients	- MRI - Sequences: T2-w, DWI, CHB-DWI, CDI	- Extracted: 416 features (*texture)* from each voxel (3 × 3 pixels) within the prostate - Selection method: minimum redundancy maximum relevance	- Classifier: support vector machine - Validation cohort: NO (leave-one-patient-out validation)	Voxel-wise detection of PCa	Histopathological sample collected after surgery	NA	- Radiomic model: T2-w: 0.58 CHB-DWI: 0.79 ADC: 0.68 CDI: 0.85 mp-MRI: 0.86	NA	9/36
(Gholizadeh et al., 2020)	N = 16, single-centre	Retrospective cohort. Biopsy proven PCa without treatment history	- MRI - Sequences: T2-w, DWI, DTI	- Extracted: 191 features (*texture*) from the whole prostate - Selection method: correlation-based features selection	- Classifier: support vector machine - Validation cohort: NO (leave-one-patient-out validation)	Voxel-wise detection of PCa	Experts' annotation on MRI images	NA	- Radiomic model: T2-w: 0.72 T2-w + DWI: 0.83 T2-w + DTI: 0.86 mp-MRI: 0.93	NA	13/36
(Monti et al., 2020)	N = 65, single-centre	Retrospective cohort. Biopsy proven PCa, PIRADS ≥ 4, PSA > 4 ng/mL	- MRI - Sequences: T2-w, ADC, DCE, DKI	- Extracted: 120 features *(first order statistic, texture)* from primary tumour and healthy tissue - Selection method: Spearman correlation, maximal information coefficient	- Classifier: Logistic regression - Validation cohort: NO	Voxel-wise detection of PCa	Experts' annotation on MRI images	NA	- Radiomic model: T2-w + ADC: 0.99 bp-MRI + DCE + DKI: 0.99	NA	10/36

(*continued on next page*)

Table 2 (*continued*)

Name, year	Data	Clinical setting	Imaging	Radiomic features	Analysis	Outcome	Ground truth	Competitive model	AUC training cohort	AUC validation cohort	RQS
(Shiradkar et al., 2016)	N = 23, Multi-centre (2)	Retrospective cohorts. Training cohort: GS ≤ 7 Validation cohort: GS ≥ 6	- MRI - Sequences: T2-w, ADC	- Extracted: 308 features (*intensity, first order statistics, co-occurrence, Gabor, texture energy*) from each voxel within the prostate - Selection method: Minimum redundancy maximum relevance	- Classifier: Quadrant discriminant analysis - Validation cohort: YES (external cohort, n = 11)	Voxel-wise detection of PCa	Experts' annotation on MRI	NA	NA	- Radiomic model: T2-w range: 0.5–0.8 T2-w + ADC range: ~ 0.4 - 0.8	11/36
(Wang et al., 2017)	N = 54, single-centre	Retrospective cohort. Biopsy proven PCa, all patients underwent radical prostatectomy	- MRI - Sequences: T2-w, DWI, DKI	- Extracted: 48 features (*shape, texture)* from dominant intraprostatic lesion and healthy area for control - Selection method: NO	- Classifier: radial basis function-support vector machine - Validation cohort: NO (leave-one-patient-out validation)	Discriminate between healthy tissue and PCa	Experts' annotation on MRI images	PIRADS	- Radiomic model: mp-MRI: 0.92 - Competitive model: PIRADS: 0.85	NA	13/36
(Bagher-Ebadian et al., 2019)	N = 117, multi-centre (2)	Retrospective cohorts. Biopsy proven PCa	- MRI - Sequences: T2-w, ADC, DWI	- Extracted: 168 features *(intensity histogram, texture, higher order statistic*) from dominant intraprostatic lesion and normal prostatic tissue - Selection method: Partial least square correlation, ANOVA	- Classifier: artificial neural network - Validation cohort: YES (two independent cohorts, one for training (N = 98) one for validation (N = 19)	Discriminate between healthy tissue and PCa	Experts' annotation on MRI images	NA	- Radiomic model: bp-MRI: 0.95	- Radiomic model: bp-MRI: 0.95	14/36
(Dulhanty et al., 2020)	N = 101, single-centre	Retrospective cohort. 72 patients PIRADS ≥ 3, among these, 41 have biopsy proven PCa, GS ≥ 6, 60 non-PCa patients	- MRI - Sequences: ADC, CHB-DWI	- Extracted: 96 features (*first order statistic*, *texture, higher order*) from each anatomical zone of the prostate - Selection method: deep learning	- Classifier: support vector machine, random forest, logistic regression - Validation cohort: NO (5-fold cross validation)	Discriminate anatomical zones with PCa from healthy tissue	Segments labelled as PCa were confirmed by biopsy	Clinical heuristics based on ADC mean, CHB-DWI value	- Radiomic model: ADC: ~ 0.90 CHB-DWI: ~ 0.90 - Competitive model: Clinical heuristics ADC: ~ 0.80 Clinical heuristics CHB-DWI: ~ 0.85	NA	12/36
(Chen et al., 2019)	N = 381, single-centre	Retrospective cohort. Biopsy report available, 182 PCa patients (GS range: 6–10), 199 non-PCa patients	- MRI	- Extracted: 781 features *(first order statistic, gradient based histogram, texture*) from 182 cancerous	- Classifier: Logistic regression	Discriminate between healthy tissue and PCa	Experts' annotation in reference to the pathological findings of the biopsy	PIRADS	- Radiomic model:	- Radiomic model:	11/36

(*continued on next page*)

Table 2 (*continued*)

Name, year	Data	Clinical setting	Imaging	Radiomic features	Analysis	Outcome	Ground truth	Competitive model	AUC training cohort	AUC validation cohort	RQS
				ROIs and 199 noncancerous prostatic tissue							
			- Sequences: T2-w, ADC	- Selection method: ANOVA, Kruskal-Wallis, univariate logistic, LASSO	- Validation cohort: YES (sample split with 7:3 ratio in training (N = 267) and validation (N = 114) cohorts)				T2-w: 0.989 ADC: 0.998 bp-MRI: 0.999	T2-w: 0.985 ADC: 0.982 bp-MRI: 0.999 - Competitive model: PIRADS: 0.867	
			- MRI	- Extracted: 2104 features (*first order statistic, texture, shape, higher order statistic*) from suspicious lesions	- Classifier: Radiomic model- random forest, competitive and combined- logistic regression				- Radiomic model:	- Radiomic model:	
(Qi et al., 2020)	N = 199, single-centre	Retrospective cohort. 85 PCa patients, GS ≥ 6, 114 non-PCa. All subjects PSA > 4 ng/mL	- Sequences: T2-w, ADC, DCE	- Selection method: variance filter assessment, t-test, Pearson correlation	- Validation cohort: YES (sample split with 2:1 ratio in training (N = 133) and validation (N = 66) cohorts)	Predict biopsy result	Histopathological sample after biopsy co-registered with MRI segmentation	Clinical factors (age, PSA, PSAD, PIRADS score, location, early enhancement)	T2-w: 0.914 ADC: 0.910 DCE: 0.793 mp-MRI: 0.945 - Competitive model: Clinical-radiological factors: 0.806 - Combined model: mp-MRI + clinical-radiological: 0.956	T2-w: 0.828 ADC: 0.853 DCE: 0.774 mp-MRI: 0.902 - Competitive model: Clinical-radiological factors: NA - Combined model: mp-MRI + clinical-radiological: 0.933	16/36
(Li et al., 2020a)	N = 381, single-centre	Retrospective cohort. Suspected PCa, biopsy results available. 142 patients csPCa, GS ≥ 7, 239 subjects healthy or GS = 6	- MRI - Sequences: T2-w, ADC	- Extracted: 396 features (*intensity, texture*) from suspicious lesions - Selection method: minimum redundancy maximum relevance, LASSO	- Classifier: Logistic regression - Validation cohort: YES (sample split in 3:2 ratio in training (N = 229) and validation (N = 152) cohorts)	Predict biopsy result	Histopathological sample after biopsy co-registered with MRI segmentation	clinical factors (age, tPSA, fPSA, PSAD, prostate volume)	- Radiomic model: bp-MRI: 0.99 - Competitive model: Clinical factors: 0.76 -Combined model: bp-MRI + clinical factors: 0.99	- Radiomic model: bp-MRI: 0.98 - Competitive model: Clinical factors: 0.79 -Combined model: bp-MRI + clinical factors: 0.98	12/36
(Hou et al., 2020)	N = 263, single-centre	Retrospective cohort. All patients with suspected PCa, PIRADS = 3. 59 patients csPCa, GS ≥ 7. 204 non-csPCa	- MRI - Sequences: T2-w, ADC, DWI	- Extracted: 1210 features *(texture)* from PIRADS evaluated lesions - Selection method: intra-class correlation > 0.9	- Classifier: support vector machine - Validation cohort: YES (sample split with 3:1 ratio in	Stratify PIRADS 3 patients into cs and non-csPCa	Lesions confirmed by biopsy	NA	NA	- Radiomic model: T2-w: 0.74 DWI: 0.82 ADC: 0.76	16/36

(*continued on next page*)

Table 2 (*continued*)

Name, year	Data	Clinical setting	Imaging	Radiomic features	Analysis	Outcome	Ground truth	Competitive model	AUC training cohort	AUC validation cohort	RQS
					training (N = 197) and validation (N = 66) cohorts)					mp-MRI: 0.89	
(Giambelluca et al., 2021)	N = 43, single-centre	Retrospective cohort. All patients with suspected PCa, PIRADS = 3. 19 patients PCa, GS ≥ 6, 24 subjects non-PCa. Pathological examination as ground truth	- MRI - Sequences: T2-w, ADC	- Extracted: 290 features (*first order statistic, texture*) from PIRADS evaluated lesions - Selection method: point-biserial correlation coefficient	- Classifier: generalized linear model, discriminant analysis - Validation cohort: NO (10-fold cross validation)	Stratify PIRADS 3 patients into cs and non-csPCa	Histopathological sample collected after surgery or biopsy	NA	- Radiomic model: T2-w: 0.78 ADC: 0.82	NA	14/36
(Algohary et al., 2018)	N = 56, single-centre	Retrospective cohort. Patients with abnormal DRE, elevated PSA, never performed prostate biopsy before. All patients under active surveillance. csPCa, GS ≥ 7	- MRI - Sequences: T2-w, DWI	- Extracted: 308 features (*first order statistic, texture*) from the whole prostate - Selection method: features different between MRI+/biopsy + and MRI-/biopsy-	- Classifier: quadrant discriminant analysis, random forest, support vector machine - Validation cohort: NO (3-fold cross validation repeated 100 times)	Detection of csPCa in patients under active surveillance	Biopsy result	NA	- Radiomic model: AUC not provided but radiomics improves PIRADS evaluation by 80 % in false negatives and 60 % in false positives	NA	12/36
(Zamboglou et al., 2020)	N = 72, multi-centre (2)	20 patients prospectively enrolled. 52 patients retrospective validation cohort. GG group range 1−5. Whole mount histopathology available for all	- PET/CT - Tracers: ^{68}Ga-PSMA-11	- Extracted: 154 (*shape, texture, higher-order statistical*) from primary tumour - Selection method: tested for inters-scanner variability	- Classifier: univariate linear model - Validation cohort: YES (sample split in training (N = 20) and validation (N = 52) cohorts)	Identification of PET invisible PCa lesions	Histopathological sample collected after surgery	NA	- Radiomic model: PET: 0.94	- Radiomic model: PET: AUC NA Sensitivity: 85 %	24/36
(Wildeboer et al., 2020)	N = 48, single-centre	Retrospective cohort. Biopsy proven PCa, all patients referred to prostatectomy	- US - Modalities: TRUS, SWE; DCE-US	- Extracted: 12 features from the whole prostate - Selection method: NO	- Classifier: Random forest - Validation cohort: NO (leave-one-patient-out validation)	Region-wise detection of PCa	Histopathological sample collected after surgery	NA	- Radiomic model: mp-US: 0.75	NA	7/36
(Domachevsky et al., 2018)	N = 22, single-centre	Retrospective cohort. Histopathologically proven PCa, GS ≥ 7	- PET/CT and PET/MR - Tracer: ^{68}Ga-PSMA11 - Sequences: T1, DWI	- They only considered standard PET parameters (SUV_{max}) and MRI (ADC) calculated in intraprostatic tumour lesion and healthy prostatic tissue	- Meann Whitney U test and Spearman correlation	Identify imaging biomarkers for PCa	Areas with PIRADS ≤ 3 were considered considered healthy tissue, PIRADS ≥ 4 PCa	NA	Conventional imaging: AUC NA, SUVmax PCa > SUV_{max} healthy tissue, ADC_{min} and ADC_{mean} PCa < healthy tissue	NA	2/36
(Orczyk et al., 2019)	N = 20, single-centre	Retrospective cohort. Suspected PCa, biopsy results available. 12 patients PCa, GS ≥ 6, 8 subjects non-PCa. csPCa: GS ≥ 7	- MRI	- Extracted: 1 value: entropy score from suspicious lesion and normal peripheral zone	- Classifier: Logistic regression	Entropy score as a biomarker for csPCa	Visual score	- Radiomic model:	NA	−3/36	

(*continued on next page*)

Table 2 (*continued*)

Name, year	Data	Clinical setting	Imaging	Radiomic features	Analysis	Outcome	Ground truth	Competitive model	AUC training cohort	AUC validation cohort	RQS
			- Sequences: T2-w, ADC, DCE	- Selection method: NO	- Validation cohort: NO			Systematic TRUS-guided biopsy combined with targeted biopsy			Entropy score: 0.89 - Competitive model: Visual score: 0.91
(Zamboglou et al., 2019)	N = 60, single-centre	20 patients prospectively enrolled for training. 40 patients retrospectively enrolled for validation. Histopathologically proven prostate adenocarcinoma	- PET - Tracers: ^{68}Ga-PSMA11	- Extracted: 133 features (*first order statistic, texture*) from primary tumour and healthy tissue - Selection method: independency from the volume	- Classifier: - - Validation cohort: two independent cohorts, training (N = 20), validation (N = 40)	Features different between PCa and non-PCA	Histopathological sample collected after surgery	NA	AUC NA, 81 % of features differ across conditions	NA	19/36
(Ginsburg et al., 2017)	N = 80, multi-centre (3)	Retrospective cohorts. Histopathologically proven PCa, GS ≥ 6	- MRI - Sequences: T2-w, ADC, DCE	- Extracted: 224 features (*first order, co-occurrence, higher order statistic*) from the whole prostate, TZ only and PZ only - Selection method: intra-class correlation, logistic regression	- Classifier: Logistic regression - Validation cohort: YES (3 independent cohorts N1 = 40, N2 = 27, N3 = 13)	Features relevant for transition and peripheral zone PCa detection	Histopathological sample collected after surgery when available	NA	- Radiomic model: TZ mp-MRI: 0.59 PZ mp-MRI: 0.70 All mp-MRI: 0.59	- Radiomic model: TZ mp-MRI: 0.57 PZ mp-MRI: 0.54 All mp-MRI: 0.57	10/36
(Xu et al., 2019)	N = 331, single-centre	Retrospective cohort. Patients with suspect PCa. Lesions with definite boundaries in MRI	- MRI - Sequences: T2-w, ADC, DWI	- Extracted: 2916 features (*texture, higher order statistic)* from suspicious lesions, normal PZ and TZ - Selection method: ICC, PCA	- Classifier: Logistic regression - Validation cohort: YES (sample split with 7:3 ratio in training (N = 232) and validation (N = 99) cohorts)	Discriminate between benign and malignant lesions	Biopsy result	Clinical factors including: age and PSA	- Radiomic model: T2-w: 0.74 DWI: 0.76 ADC: 0.87 bp-MRI: 0.89 - Competitive model: Clinical factors: 0.75 - Combined models: bp-MRI + clinical factors: 0.91	- Radiomic model: T2-w: 0.81 DWI: 0.78 ADC: 0.89 bp-MRI: 0.92 - Competitive model: Clinical factors: 0.73 - Combined models: bp-MRI + clinical factors: 0.93	15/36

Summary of the studies investigating the utility of radiomics for the detection of PCa. GS = Gleason score; NA = not available, ANOVA = analysis of variance; PIRADS = Prostate Imaging-Reporting And Data Systems; LASSO = least Absolute Shrinkage and Selection Operator; PSA = Prostatic Specific Antigen; US = Ultrasound; ICC = Intra Cluster Correlation; TZ = Transition zone, PZ = Peripheral zone; PCA = Principal Component Analysis. Reported results refer to the classifier that yielded the highest AUC in the study, RQS = Radiomics Quality Score.

Table 3
Radiomics to assess the clinical relevance of PCa.

Name, year	Data	Clinical setting	Imaging	Radiomic features	Analysis	Outcome	Ground truth	Competitive model	AUC training cohort	AUC validation cohort	RQS
(Abdollahi et al., 2019a)	N = 33, single-centre	Retrospective. Patients with biopsy proven primary prostate adenocarcinoma, treated with IMRT. MRI collected prior to treatment	- MRI - Sequences: T2-w, ADC	- Extracted: 4540 features (*shape, texture*) from the primary tumour - Selection method: Chi-squared, ANOVA, select from model, variance threshold	- Classifier: Linear support vector machine, logistic regression, adaptive boost, decision tree, gaussian naïve Bayesian, K-nearest neighbour, Bernoulli naïve Bayesian, stochastic gradient descent, random forest - Validation cohort: NO (10-fold cross validation)	GS ≤ 7 vs GS ≥ 8	GS defined after biopsy	NA	T2-w: 0.739	NA	17/36
(Gong et al., 2020)	N = 489, single-centre	Retrospective cohort. PCa diagnosed by pathology. MRI collected before pathological examination	- MRI - Sequences: T2-w, DWI	- Extracted: 1345 features (*first order statistic, shape, texture*) from the whole prostate - Selection method: Sequential backward elimination	- Classifier: Logistic regression - Validation cohort: YES (sample split with 2:1 ratio in training (N = 326) and test (N = 163) cohorts)	GS ≤ 7 vs GS ≥ 8	GS defined after biopsy or after RP when performed	Combination of PSA and PSAD levels	- Radiomic model: T2-w: 0.712 DWI: 0.80 bp-MRI: 0.81 - Competitive model: Clinical: 0.696 - Combined models: bp-MRI + clinical factors: 0.81	- Radiomic model: T2-w: 0.645 DWI: 0.787 bp-MRI: 0.788 - Competitive model: Clinical: 0.72 - Combined models: Bp-MRI + clinical factors: 0.78	11/36
(Hectors et al., 2019)	N = 64, single-centre	Retrospective cohort. PCa Patients treated with RP. MRI collected within 6 months prior to operation	- MRI - Sequences: T2-w, ADC	- Extracted: 224 features (*first order statistic, texture*) from primary tumour - Selection method: LASSO	- Classifier: Logistic regression - Validation cohort: NO (nested cross validation)	GS ≤ 7 vs GS ≥ 8	GS defined after RP	NA	T2-w: 0.72 ADC: 0.57 bp-MRI: 0.65	NA	13/36
(Tanadini-Lang et al., 2018)	N = 41, single-centre	Retrospective cohort. Biopsy confirmed PCa, CT scan before RP	- CT	- Extracted: 1701 features (*first order statistic, texture, wavelet transformation*) from the whole prostate - Selection method: PCA, and for each independent component retrieve the one that correlates the most with outcome	- Classifier: Logistic regression - Validation cohort: NO (10-fold cross validation)	GS ≤ 7 vs GS ≥ 8	GS defined after biopsy	NA	CT: 081	NA	9/36
(Liu et al., 2019)	N = 40, single-centre	Retrospective cohort. Pathology confirmed PCa. PIRADS 4–5	- MRI	- Extracted: 1029 features (*shape, first order statistic, texture, higher order statistic*) from the primary tumour	- Classifier: Linear support vector machine, logistic regression, random forest, decision tree, K-nearest neighbour	GS ≤ 7 vs GS ≥ 8	GS defined after biopsy	NA	DCE-first: 0.88	NA	12/36

(*continued on next page*)

Table 3 (*continued*)

Name, year	Data	Clinical setting	Imaging	Radiomic features	Analysis	Outcome	Ground truth	Competitive model	AUC training cohort	AUC validation cohort	RQS
(Zamboglou et al., 2019)	N = 60, single-centre	Prospective cohort. Histopathologically proven adenocarcinoma of the prostate and intended RP. Retrospective cohort for validation	- Sequences: DCE first and strongest phase - PET/CT - Tracer: ^{68}Ga-PSMA	- Selection method: Chi-squared, LASSO - Extracted: 133 features (*first order statistic, texture*) from primary tumour - Selection method: Robustness, interdependency with volume	- Validation cohort: NO (5-fold cross validation) - Classifier: Logistic regression - Validation cohort: YES (40 patients enrolled retrospectively) - ROI identified by 1) expert in images and 2) according to histopathology	GS ≤ 7 vs GS ≥ 8	GS defined after RP	NA	DCE-strongest: 0.84 Combined phases DCE: 0.93 PET-expert: 0.91 PET-histology: 0.93	PET-expert: 0.84	17/36
(Algohary et al., 2020)	N = 231, multi-centre (4)	Retrospective cohort. Biopsy confirmed PCa.	- MRI - Sequences: T2-w, DWI	- Extracted: 300 intra-tumoral and 1200 peri-tumoral features (*first order statistic, texture)* from the primary tumour and peri-tumoral regions - Selection method: Minimum redundance maximum relevance	- Classifier: Quadratic discriminant analysis - Validation cohort: YES (sample split with 1:1 ratio in training (N = 116) and validation (N = 115) cohorts)	D'Amico risk classification system, low vs high risk	D'Amico risk classification	NA	- Peri-tumoral: T2-w: 0.73 ADC: 0.71 bp-MRI: 0.87 - Intra-tumoral: T2-w: 0.79 ADC: 0.80 bp-MRI: 0.87 - Intra + peri-tumoral: bp-MRI: 0.95	- Peri-tumoral: T2-w: 0.71 ADC: 0.76 bp-MRI: 0.84 - Intra-tumoral: T2-w: 0.71 ADC: 0.79 bp-MRI: 0.81 - Intra + peri-tumoral: bp-MRI: 0.87	13/36
(Bleker et al., 2020)	N = 206, single-centre	Prospective cohort. PIRADS 3–5. Biopsy results available for all participants	- MRI - Sequences: T2-w, DWI, DCE	- Extracted: 92 features *(first order statistic, texture)* from the dominant intraprostatic lesion - Selection method: Machine learning, clinical experience, and domain knowledge	- Classifier: Random forest, extreme gradient boosting - Validation cohort: YES (sample split with ratio 4:3 in training (N = 130) and validation (N = 76) cohorts)	GS ≤ 6 vs GS ≥ 7	GS defined after biopsy	NA	T2-w + DWI: 0.80 mp-MRI: 0.87	T2-w + DWI: 0.81 mp-MRI: 0.87	15/36
(Chaddad et al., 2018a)	N = 99, online database	Online database of images with GS available (SPIE-AAPM-NCI prostate MR Gleason Grade Group challenge)	- MRI - Sequences: T2-w, ADC	- Extracted: 41 features (*intensity, texture)* from primary tumour - Selection method: Kruskal-Wallis, Spearman correlation	- Classifier: Random forest - Validation cohort: YES (5-fold cross validation and sample split with 2:1 ratio in training (N = 40)	GS ≤ 6 vs GS ≥ 7	GS provided by SPIE-AAPM-NCI prostate MR Gleason Grade Group challenge	NA	bp-MRI: 0.83	bp-MRI: 0.89	11/36

(*continued on next page*)

Table 3 (*continued*)

Name, year	Data	Clinical setting	Imaging	Radiomic features	Analysis	Outcome	Ground truth	Competitive model	AUC training cohort	AUC validation cohort	RQS
					and validation (N = 20) cohorts)						
			- MRI	- Extracted: 57 features (*texture)* from the primary tumour	- Classifier: Random forest					JIM: 0.78	
(Chaddad et al., 2018b)	N = 99, online database	Online database of images with GS available (SPIE-AAPM-NCI prostate MR Gleason Grade Group challenge)	- Sequences: T2-w, ADC	- Selection method: Kruskal-Wallis, Spearman correlation	- Validation cohort: (5-fold cross validation and sample split with 2:1 ratio in training (N = 40) and validation (N = 20) cohorts)	GS ≤ 6 vs GS ≥ 7	GS provided by SPIE-AAPM-NCI prostate MR Gleason Grade Group challenge	NA	NA	ADC: 0.68	11/36
					- Joint intensity matrices (JIM) to combine T2-w and ADC features					T2-w: 0.66 JIM + bp-MRI: 0.78	
Gugliandolo et al., 2021)	N = 49, single-centre	Retrospective cohort. Patients with localized PCa treated with RT. MRI collected prior to therapy	- MRI	- Extracted: 1058 features (*shape, intensity, texture)* from the whole prostate	- Classifier: Multivariate logistic regression	GS ≤ 6 vs GS ≥ 7	GS defined after biopsy	NA	T2-w: 0.75	NA	11/36
			- Sequences: T2-w	- Selection method: Kruskal-Wallis, Spearman correlation	- Validation cohort: NO (leave one patient out validation)						
			- MRI	- Extracted: 232 features (*first order statistic, texture*) from dominant intraprostatic lesion	- Classifier: Logistic regression, support vector machines, random forest, XGboost, convolutional neural network				- Radiomic model:	- Combined model:	
(Woźnicki et al., 2020)	N = 191, multi-centre (2)	Retrospective cohort. Suspect of PCa, biopsy results available	- Sequences: T2-w, ADC	- Selection method: Minimum redundancy maximum relevance	- Validation cohort: YES (sample split in training (N = 151) and validation (N = 40) cohorts)	GS ≤ 6 vs GS ≥ 7	GS defined after biopsy	Clinical factors including PSAD, PIRADS, DRE	bp-MRI: 0.807 - Competitive model: PIRADS: 0.681 PSAD: 0.644 DRE: 0.666 Mean ADC: 0.697	bp-MRI + clinical factors + PIRADS: 0.844 - Competitive model: PIRADS: 0.688 Mean ADC: 0.571	13/36
(Deukwoo et al., 2018)	N = 344, online database	Online database (SPIE-AAPM-NCI prostate MR Gleason Grade Group challenge) all images used because they participated in the challenge	- MRI - Sequences: T2-w, DCE, DWI, PD-w	- Extracted: 216 features (*shape, first order statistic, texture*) from primary tumour - Selection method: Decision tree, random forest, LASSO	- Classifier: Logistic regression - Validation cohort: YES (sample split with 3:2 ratio in training (N = 204) and validation (N = 140) cohorts)	GS ≤ 6 vs GS ≥ 7	GS provided by SPIE-AAPM-NCI prostate MR Gleason Grade Group challenge	NA	NA	mp-MRI: 0.82	11/36
(Parra et al., 2018)	N = 68, multi-centre (2)	Retrospective cohorts. Biopsy confirmed PCa	- MRI - Sequences: DCE	- Extracted: 7 features from the DCE time activity curves - Selection method: They used each feature	- Classifier: Decision tree - Validation cohort: YES (two separate cohorts,	GS ≤ 6 vs GS ≥ 7	GS after biopsy	NA	DCE: 0.88	DCE: 0.76	10/36

(*continued on next page*)

Table 3 (*continued*)

Name, year	Data	Clinical setting	Imaging	Radiomic features	Analysis	Outcome	Ground truth	Competitive model	AUC training cohort	AUC validation cohort	RQS
				alone or paired with another one	training N = 38, validation N = 30)						
(Toivonen et al., 2019)	N = 62, single-centre	Histologically confirmed PCa. Patients scheduled for prostatectomy	- MRI - Sequences: T2-w, DWI, ADC	- Extracted: 1281 features (*texture)* from the primary tumour - Selection method: 10% more associated with outcome, top 1% for mp-MRI analysis	- Classifier: Logistic regression - Validation cohort: NO (nested cross validation)	GS ≤ 6 vs GS ≥ 7	GS defined after RP	NA	T2-w: 0.80 ADC: 0.76 DWI: 0.78 T2: 0.56 mp-MRI: 0.88	NA	14/36
(Bonekamp et al., 2018)	N = 316, single-centre	Retrospective cohort. Suspect PCa, biopsy results available. No previous treatment history	- MRI - Sequences: T2-w, ADC	- Extracted: 846 features (*first order statistic, volume, shape, texture)* from all suspicious lesions - Selection method: Univariate feature selection	- Classifier: Random forest - Validation cohort: YES (sample split with 4:3 ratio in training (N = 183) and validation (N = 133) cohorts)	GG < 2 vs GG ≥ 2	GG defined after biopsy	Mean ADC	- Radiomic model: bp-MRI: 0.78 - Competitive model: Mean ADC: 079	- Radiomic model: bp-MRI: 0.88 - Competitive model: Mean ADC: 084	5/36
			- MRI	- Extracted: (*first order statistic, shape, texture)* from the primary tumour	- Classifier: Support vector machine, artificial neural network, random forest	GG < 3 vs GG ≥ 3	GS defined after biopsy	PIRADS	NA	- Radiomic model: ADC: ~ 0.65 - Competitive model: PIRADS: ~ 0.75 - Combined model: ADC + PIRADS: ~ 0.80	
(Bernatz et al., 2020)	N = 73, single-centre	Retrospective cohort. 35 patients csPCa, defined as GG group ≥ 3. 38 patients non-csPCa.	- Sequences: ADC	- Selection method: iterative Wilcoxon and t-test	- Validation cohort: YES (sample split with rate 7:3 in training (N = 51) and validation (N = 22) cohorts, repeated 100 times)						12/36
(McGarry et al., 2019)	N = 48, single-centre	Prospective cohort. PCa patients scheduled for RP	- MRI - Sequences: T2-w, ADC, DCE	- Extracted: 81 radiomic profiles from the whole prostate - Selection method: NO	- Classifier: Linear models - Validation cohort: NO	GG < 4 vs GG ≥ 4	GG defined after RP	NA	mp-MRI: 0.77	NA	17/36
(Papp et al., 2020)	N = 52, single-centre	Retrospective cohort of patients with localized PCa that underwent RP	- PET/MRI - Tracers: ^{68}Ga-PSMA11 - Sequences: T2-w, ADC	- Extracted: 442 features from the primary tumour - Selection method: Pearson correlation	- Classifier: Random forest - Validation cohort: NO (Monte Carlo cross validation: 1000 folds)	GG < 4 vs GG ≥ 4	GS defined after RP	SUV_{max}, SUV_{peak}, SUV_{tlg}, volume	- Radiomic model: PET/MRI: 0.86 - Competitive model: SUV_{max}: 0.80 SUV_{peak}: 0.74 SUV_{tlg}: 0.64 Volume: 0.53	NA	20/36
(Brunese et al., 2019)			- MRI	- Extracted: 71 features (*first order statistic,*	- Classifier: Timed automata	GS inference	GS defined after biopsy	NA	T2-w: 1	NA	0/36

(*continued on next page*)

Table 3 (*continued*)

Name, year	Data	Clinical setting	Imaging	Radiomic features	Analysis	Outcome	Ground truth	Competitive model	AUC training cohort	AUC validation cohort	RQS
	N = 36, online database	Online database publicly available on cancer imaging archive		*shape, texture)* from the whole prostate - Selection method: NO	- Validation cohort: NO						
(Brunese et al., 2020)	N = 62, online database	Data from two online databases publicly available at cancer imaging archive	- Sequences: T2-w	- MRI	- Extracted: 71 features (*first order statistic, shape, texture*) from the whole prostate	- Classifier: Random forest, convolutional neural network, support vector machines, artificial neural network	GS inference	GS defined after biopsy	NA	T2-w: 0.97	NA
- Sequences: T2-w	- Selection method: NO	- Validation cohort: NO (5-fold cross validation)	9/36								
(Chaddad et al., 2020)	N = 99, online database	Online database of images with GS available (SPIE-AAPM-NCI prostate MR Gleason Grade Group challenge)	- MRI - Sequences: T2-w, ADC, DCE	- Extracted: 7857 features (*deep entropy*) from an 84 × 84 pixel area containing the lesion - Selection method: Spearman correlation	- Classifier: Random forest - Validation cohort: YES (5-fold cross validation and then sample split with 7:3 ratio in training (N = 70) and validation (N = 29) cohorts repeated 20 times)	GS inference	GS defined after biopsy	NA	mp-MRI: 0.87	mp-MRI: 0.89	12/36
(Osman et al., 2019)	N = 362, single-centre	Retrospective cohort. Patients with localized PCa, treated with RT.	- CT	- Extracted: 1618 features (*first order statistic, texture)* from the whole prostate - Selection method: LASSO, elastic net	- Classifier: generalized linear model - Validation cohort: YES (sample split with ratio 4:1 in training (N = 290) and validation (N = 72) cohorts)	1) GS ≤ 3 + 4 vs GS ≥ 4 + 3 And 2) GS ≤ 6 vsGS > 6 And 3) GS ≤ 7 vs GS > 7	GS defined after biopsy	NA	1) CT: 0.97 2) CT: 0.90 3) CT: 0.67	1) CT: 0.65 2) CT: 0.60 3) CT: 0.70	12/36
(Cuocolo et al., 2019)	N = 75, single-centre	Retrospective cohort. Histopathologically confirmed PCa, with PIRADS ≥ 3	- MRI - Sequences: T2-w, ADC, DWI	- Extracted: 30 features (*shape)* from the primary tumour - Selection method: univariable logistic regression	- Classifier: multivariate logistic regression - Validation cohort: NO	GS ≤ 3 + 4 vs GS ≥ 4 + 3	GS defined after biopsy	NA	ADC: 0.78	NA	4/36
(Zhang et al., 2020a)	N = 159, multi-centre (2)	Retrospective cohort. Biopsy proven PCa. No previous treatment history	- MRI - Sequences: T2-w, DWI, ADC	- Extracted: 1188 features (*first order statistic, texture)* from the primary tumour - Selection method: minimum redundancy maximum relevance, LASSO	- Classifier: multivariate logistic regression - Validation cohort: YES (two separate cohorts, training N = 76 and validation N = 83)	GS ≤ 3 + 4 vs GS ≥ 4 + 3	GS defined after biopsy	ADC e PSA level	- Radiomic model: mp-MRI: 0.86 - Competitive model: PSA: 0.91 - Combined model:	- Radiomic model: mp-MRI: 0.81 - Competitive model: PSA: 0.69 - Combined model:	16/36

(*continued on next page*)

Table 3 (*continued*)

Name, year	Data	Clinical setting	Imaging	Radiomic features	Analysis	Outcome	Ground truth	Competitive model	AUC training cohort	AUC validation cohort	RQS
(yang et al., 2020)	N = 166, single-centre	Retrospective cohort. Patients with localized PCa who underwent RP. MRI collected prior to therapy	- MRI - Sequences: T2-w, ADC, DCE	- Extracted: 4404 features (*shape, first order statistic, texture, higher order statistic*) from the primary tumour - Selection method: Mutual information maximization	- Classifier: Logistic regression - Validation cohort: YES (sample split in training (N = 116) and validation (N = 50) cohorts)	GS upgrade from biopsy to surgery	GS defined after RP	Time between biopsy and surgery	mp-MRI + ADC: 0.93 - Radiomic model: T2-w: 0.74 DCE: 0.72 ADC: 0.81 mp-MRI: 0.89 - Competitive model: Clinical factors: 0.67 - Combined model: mp-MRI + clinical factors: 0.91	mp-MRI + ADC: 0.84 - Radiomic model: T2-w: 0.70 DCE: 0.73 ADC: 0.76 mp-MRI: 0.87 - Competitive model: Clinical factors: 0.65 - Combined model: mp-MRI + clinical factors: 0.91	15/36

Summary of the studies investigating the utility of radiomics to assess the clinical relevance of PCa. IMRT = Intensity Modulated Radiation Therapy; ANOVA = Analysis of Variance; GS = Gleason score; NA = not available; PSA = Prostatic Specific Antigen, PSAD = Prostatic Specific Antigen Density; LASSO = least Absolute Shrinkage and Selection Operator; PIRADS = Prostate Imaging-Reporting And Data Systems; GG = Gleason grade. Reported results refer to the classifier that yielded the highest AUC in the study, RQS = radiomics quality score.

Table 4
Radiomics to predict BCR following definitive therapy.

Name, year	Data	Clinical setting	Imaging	Radiomic features	Analysis	Outcome	Ground truth	Competitive model	AUC training cohort	AUC validation cohort	RQS
(Bourbonne et al., 2019)	N = 107, single-centre	Retrospective cohort. Histopathologically proven PCa. 24 months follow-up (or BCR) treated with RP. Exclusion criteria: adjuvant therapy, post-operative PSA ≥ 4 ng/mL	- MRI - Sequences: T2-w, ADC	- Extracted: 27,376 features (*texture, higher order statistic)* from the primary tumour - Selection method: aggressive false discovery reduction, Pearson correlation, robustness score	- Classifier: Cox regression - Validation cohort: YES (sample split with 2:1 ratio in training (N = 70) and validation (N = 37) cohorts)	Biochemical recurrence prediction Defined as a PSA increase above 0.2 ng/ml confirmed on two successive blood samples	BCR ADC: 0.799 - Competitive model: Clinical factors: 0.76 - Combined models: ADC + clinical factors: 0.85	Clinical factors: GS, pre/post operative PSA, T stage, margin status, age, CAPRA-S score	- Radiomic model: ADC: 0.76 - Competitive model: Clinical factors: 0.56 - Combined models: ADC + clinical factors: 0.52	- Radiomic model:	16/36
(Dinis Fernandes et al., 2018)	N = 120, single-centre	Retrospective cohort of patients treated with external-beam radiotherapy. 5 years follow-up	- MRI - Sequences: T2-w	- Extracted: 254 features (*texture*) from the whole prostate - Selection method: minimum redundancy maximum relevance, Pearson correlation	- Classifier: Random forest, logistic regression - Validation cohort: NO (10-fold cross validation)	Biochemical recurrence prediction	BCR defined according to the Phoenix criteria	Clinical factors: PSA, GS, tumour staging	- Radiomic model: T2-w: 0.63 - Competitive model: Clinical factors: 0.51 - Combined models: T2-w + clinical factors: 0.56	NA	11/36
(Bourbonne et al., 2020)	N = 195, multi-centre (2)	Retrospective cohort. Histopathologically proven PCa, treated with RP. Exclusion criteria: adjuvant therapy, post-operative PSA ≥ 4 ng/mL	- MRI - Sequences: T2-w, ADC	- Extracted: 27376 features (*texture, higher order statistic)* from the primary tumour - Selection method: Only ADC SZE_{GLSZM} was considered	- Classifier: Cox regression - Validation cohort: YES (two independent cohorts, one for training (N = 107), one for validation (N = 88)	Biochemical recurrence prediction	BCR Defined as a PSA increase above 0.2 ng/mL confirmed on two successive blood samples	Clinical factors: GS, pre/post operative PSA, T stage, margin status, age, CAPRA-S score	- Radiomic model: ADC: 0.82 - Competitive model: Clinical factors: 0.64 - Combined models: ADC + clinical factors: 0.84	- Radiomic model: ADC: 0.76 - Competitive model: Clinical factors: 0.56 - Combined models: ADC + clinical factors: 0.67	17/36
(Shiradkar et al., 2018)	N = 120, multi-centre (2)	Retrospective cohort. Patients treated with RT or RP. Cohort followed for 3 years. 42 patients showed BCR, 78 non-BCR	- MRI - Sequences: T2-w, ADC	- Extracted: 600 features (*first order statistic, texture, higher order statistic*) from the dominant intraprostatic lesion - Selection method: minimum redundancy maximum relevance,	- Classifier: random forest, support vector machine, linear discriminant analysis - Validation cohort: YES (two independent cohorts, one for	Biochemical recurrence prediction	BCR defined as 2 consecutive readings of PSA > 0.2 ng/ml after RP, and as an increase in PSA > 2 ng/ml compared to the initial PSA nadir value after RT	NA	ADC: 0.84	ADC: 0.73	14/36

(*continued on next page*)

Table 4 (*continued*)

Name, year	Data	Clinical setting	Imaging	Radiomic features	Analysis	Outcome	Ground truth	Competitive model	AUC training cohort	AUC validation cohort	RQS
				joint mutual information, conditional mutual information	training (N = 70), one for validation (N = 50)						
(Zhong et al., 2020)	N = 91, single-centre	Retrospective cohort. Patients with confirmed prostate carcinoma treated with RT. 1o years follow-up	- MRI - Sequences: T1, T2, DWI	- Extracted: 1536 features (*pixel level, object level, semantic level)* from the whole prostate - Selection method: K-PCA	- Classifier: Adaboost model - Validation cohort: YES (sample split with 4:1 ratio in training (N = 73) and validation (N = 18) cohorts)	Biochemical recurrence prediction	BCR defined according to the Phoenix criteria	NA	mp-MRI: 0.99	mp-MRI: 0.73	11/36
(Bosetti et al., 2020)	N = 31, single-centre	Retrospective cohort. Patients with localized prostate adenocarcinoma treated with RT. 5 years follow-up	- CBCT	- Extracted: 31 features (*histogram based, shape, size)* from the whole prostate - Selection method: concordance correlation coefficient	- Classifier: Logistic regression - Validation cohort: NO (3-fold cross validation repeated 10 times)	Biochemical recurrence prediction	BCR defined according to the Phoenix criteria	NA	CBCT: 1	NA	11/36
(Gnep et al., 2017)	N = 74, single-centre	Retrospective cohort. Patients with localized prostate adenocarcinoma treated with RT. 5 years follow-up	- MRI - Sequences: T2-w, ADC	- Extracted: 144 features (*geometrical, first order statistic, gradient, texture*)from the primary tumour and whole prostate - Selection method: random survival forest	- Classifier: Cox proportional hazard model - Validation cohort: NO	Biochemical recurrence prediction	BCR defined according to the Phoenix criteria	NA	AUC not provided. Including top 5 features C-index: 0.9	NA	5/36
(Li et al., 2020b)	N = 198, multi-centre (4)	Retrospective cohort. Median follow-up: 35 months. Patients with localized PCa treated with RP. No history of adjuvant or neoadjuvant therapies.	- MRI - Sequences: T2-w, ADC	- Extracted: 200 features (*first order statistic, texture*) from the primary tumour - Selection method: Pearson correlation, test-retest, minimum redundancy maximum relevance	- Classifier: Cox proportional hazard model - Validation cohort: YES (two independent cohorts, one for training (N = 71), one for validation (N = 127))	Biochemical recurrence prediction	BCR defined as 2 consecutive readings of PSA > 0.2 ng/mL after RP	Decipher, CAPRA, CAPRA-S	NA	- Radiomic model: bp-MRI: 0.71 - Competitive model: CAPRA: 0.69 Decipher: 0.66	19/36
(Papp et al., 2020)	N = 52, single-centre	Prospective cohort. Mean follow-up 41 months	- PET/MRI - Tracers: ^{68}Ga-PSMA11 - Sequences: T2-w, ADC	- Extracted: 442 features from the primary tumour - Selection method: Pearson correlation	- Classifier: Random forest - Validation cohort: NO (Monte Carlo cross validation: 1000-fold)	Biochemical recurrence prediction	BCR defined as 2 consecutive readings of PSA > 0.2 ng/ml after RP	PSA, Enumerated clinical stage	- Combined model: PET/MRI + PSA + stage: 0.90	NA	20/36

Summary of the studies investigating the utility of radiomics to predict the risk of biochemical recurrence following definitive therapy in PCa. BCR = biochemical recurrence; PSA = Prostatic specific Antigen; GS = Gleason score; NA = Not Available; RP = radical prostatectomy; RT = Radiation Therapy; K-PCA = Kernel-Principal Component Analysis. Reported results refer to the classifier that yielded the highest AUC in the study, RQS = Radiomics Quality Score.

Table 5
Radiomics to predict RT outcome and to monitor treatment efficacy.

Name, year	Data	Clinical setting	Imaging	Radiomic features	Analysis	Outcome	ground truth	Competitive model	AUC training cohort	AUC validation cohort	RQS
(Abdollahi et al., 2019a)	N = 33, single-centre	Prospective cohort. Patients with biopsy proven prostate adenocarcinoma that never had prostate surgery	- MRI - Sequences: T1-w, T2-w, DWI, ADC	- Extracted: 4540 features (*texture, intensity, histogram, shape*) from the primary tumour - Selection method: ANOVA, variance threshold, selection from model, χ^2	- Classifier: Linear support vector machine, logistic regression, Bernoulli naïve bayes, stochastic gradient descent, K-nearest neighbour, decision tree, random forest, adaptive boosting, gaussian naïve bayes - Validation cohort: NO	Identify IMRT responders	Change of at least 20 % in ADC values before and after IMRT	NA	T2-w: 0.77 ADC: 0.78	NA	17/36
(Wu et al., 2019)	N = 23, single-centre	Retrospective cohort. Patients with biopsy proven PCa that had MR scan within a month prior to RT initiation	- MRI - Sequences: T1-w, T2-w, DCE, ADC	- Extracted: 26,601 features (*first order statistical, shape, texture, filter-based)* from the primary tumour - Selection method: ICC	- Classifier: SVM - Validation cohort: NO (leave one patient out)	Identify RT responders	PSA $\leq$ 0.5 after treatment considered responders	NA	T2-w: 0.67 ADC: 0.79 ADC + T2-w: 0.88	NA	11/36
(Brunese et al., 2019)	N = 36, From publicly available Cancer Imaging Archive	NA	- MRI - Sequences:	- Extracted: 71 features (*first order statistics, texture*) from primary tumour - Selection method: NO	- Classifier: Timed automata network - Validation cohort: NO	Predict suggested treatment	NA	NA	AUC not provided. Specificity: 0.94 Sensitivity: 1	NA	−3/36
(Lee et al., 2019)	N = 59, single-centre	Prospective cohort. Patients enrolled in a tumour dose escalation trial (simultaneous integrated boost or high dose rate brachytherapy)	- MRI - Sequences: T2-w, ADC	- Extracted: 101 features (*first order statistic, texture)*from the primary tumour - Selection method: NO	- Classifier: t-test - Validation cohort: NO	Identify early responses and adaptation to RT	NA	NA	AUC not provided, 44 RF changed over time	NA	2/36
(Lorenz et al., 2019)	N = 4, single-centre	Prospective cohort. 4 weeks monitoring of patients undergoing IMRT	- MRI - Sequences: T2-w	- Extracted: 30 features (*First order statistical*) from prostate, rectum and bladder - Selection method: NO	- Classifier: linear mixed effects regression - Validation cohort: NO	Delta radiomics as biomarker for treatment efficacy /toxicity	NA	NA	AUC not provided, 5 RF changed over time	NA	6/36
(Abdollahi et al., 2019b)	N = 33, single-centre	Prospective cohort. Patients with biopsy proven prostate cancer scheduled for IMRT	- MRI - Sequences: T1-w, T2-w, DWI	- Extracted:274 features (*histogram, gradient, run-length matrix, co-occurrence matrix, autoregressive, wavelet*) from the bladder - Selection method: NO	- Classifier: Logistic regression - Validation cohort: NO	Identify subjects at risk for radiation-induced urinary toxicity	Urinary toxicity: grade $\geq$ 2 urinary toxicity	NA	Range: 0.51 – 0.75	NA	4/36

(*continued on next page*)

Table 5 (*continued*)

Name, year	Data	Clinical setting	Imaging	Radiomic features	Analysis	Outcome	ground truth	Competitive model	AUC training cohort	AUC validation cohort	RQS
(Mostafaei et al., 2020)	N = 64, single-centre	Prospective cohort. Patients with pathologically confirmed PCa candidate to external beam radiotherapy. Use pre-treatment CT	- CT	- Extracted: 109 features (*first order statistical, shape, texture)* from rectal and bladder walls - Selection method: stacking algorithm and elastic net penalized logistic regression - Extracted: 42 features (*texture)* from rectum and bladder	- Classifier: ANN, random forest and SVM as base learners and elastic net logistic regression as meta-learner - Validation cohort: NO (100 times 5-fold cross-correlation) - Classifier: multivariate logistic regression	Identify patients at risk for developing cystitis and proctitis	Cystitis: grade ≥ 1 radiation induced Proctitis: grade ≥ 1 radiation induced	Clinical factors (PSA, prostate volume, GS, dose volume, planning target volume, age)	- Radiomic model: cystitis: 0.71 proctitis: 0.71 - Competitive model: cystitis: 0.67 proctitis: 0.66 - Combined models: Cystitis: 0.77 Proctitis: 0.65	NA	18/36
(Rossi et al., 2018)	N = 351, multi-centre	Retrospective cohort from HYPRO trial	3D dose distribution	- Selection method: univariate logistic regression, Spearman rank test	- Validation cohort: NO	Onset of several adverse effects induced by RT	Nocturia if urinary night frequency was P4 and rectal bleeding if laser treatment or transfusion was required	Non-treatment related parameters + dose volume histogram	Competitive model: Faecal incontinence: 0.68 Nocturia: 0.63 Urinary incontinence: 0.71 Rectal bleeding: 0.68 - Combined models: Faecal incontinence: 0.75 Nocturia: 0.67 Urinary incontinence: 0.73 Rectal bleeding: 0.72	NA	11/36
(Tsang et al., 2020)	N = 10, single-centre	Retrospective cohort. Histologically confirmed PCa, stage range: from T1 to T3b	- MRI - Sequences: T2-w	- Extracted: 3 features (*texture)* from the prostate and urethra - Selection method: NO	- Classifier: Wilcoxon-signed rank test - Validation: NO	Identify patients at risk for urethral stricture	A stricture was defined by a patient requiring dilatation or catheterization for stricture confirmed on cystoscopy.	NA	AUC not provided. Contrast and homogeneity features are different in patients who developed urethral stricture	NA	3/36

Summary of the studies investigating the utility of radiomics for the prediction of radiation therapy outcome and for monitoring treatment efficacy in PCa. ANOVA = Analysis Of Variance; IMRT = Intensity Modulated Radiation Therapy; NA = Not Available; RF = Radiomic Features; ANN = Artificial Neural Network; SVM = Support Vector Machine; ICC = Intra Cluster Correlation; RT = Radiation Therapy. Reported results refer to the classifier that yielded the highest AUC in the study, RQS = Radiomics Quality Score.

Table 6
Radiomics to detect distant metastases and detect lymph node infiltrations.

Name, year	Data	Clinical setting	Imaging	Radiomic features	Analysis	Outcome	Ground truth	Competitive model	AUC training cohort	AUC validation cohort	RQS
(Moazemi et al., 2020)	N = 72, single-centre	Retrospective cohort. Histologically confirmed PCa, GS ≥ 6. All patients underwent previous treatments	- PET/CT - Tracers: ^{68}Ga-PSMA11	- Extracted: 40 features (*first order statistic, higher order statistic, texture, shape, volumetric zone and run length*) from all PSMA avid hotspots - Selection method: NO (they considered PET only, CT only, PET/CT)	- Classifier: linear support vector machine, radial basis function support vector machine, polynomial kernel support vector machine, extra trees, random forest - Validation cohort: YES (sample split with 2:1 ratio in training (N = 48) and validation (N = 24) cohorts)	Metastases and lymph nodes infiltration detection	Experts' classification looking at imaging	NA	PET: 0.92 CT: 0.98 PET/CT: 0.98	PET: 0.90 CT: 0.97 PET/CT: 0.98	4/36
(Wuestemann et al., 2020)	N = 149, single-centre	Retrospective cohort. They considered multiple pathologies, PCa included	- BS	- Extracted: BSI - Selection method: NO	- Classifier: artificial neural network - Validation cohort: NO	Bone metastases detection	Experts' classification looking at imaging	NA	BSI: 0.94	NA	0/36
(Filograna et al., 2019)	N = 1, single-centre	Retrospective cohort. They considered multiple pathologies, PCa included. Pre-treatment MR images of patients with diagnosed bone marrow metastasis	- MRI - Sequences: T1, T2	- Extracted: 89 features (*histogram, morphological, texture)* from vertebral bodies - Selection method: Wilcoxon test	- Classifier: logistic regression - Validation cohort: NO	Bone metastases detection	Radiologist classification	NA	T1: 0.81 T2: 0.91	NA	6/36
(Giesel et al., 2017)	N = 40, single-centre	Retrospective cohort. Imaging performed before therapy initiation according to clinical schedule. Patients that already underwent intervention were excluded	- PET/CT - Tracers: ^{68}Ga-PSMA11	- Extracted: They used classical PET/CT parameters, investigating lymph nodes - Selection method: NO	- Classifier: NO - Validation cohort: NO	Lymph nodes infiltration detection	SUV_{max} LN > 3 times SUV_{max} blood	NA	CT: 0.92	NA	NA
(Peeken et al., 2020)	N = 80, multi-centre (2)	Retrospective cohort. Patients with recurrent PCa, positive lymph nodes, after radical prostatectomy	- PET/CT -Tracers: ^{68}Ga-PSMA11	- Extracted: 156 features (*shape, first order statistic, texture)* from lymph nodes - Selection method: LASSO	- Classifier: Logistic regression - Validation cohort: YES (two independent cohorts, one for training (N = 47) one for validation (N = 33)	Lymph nodes infiltration detection	Histology confirmed lymph node infiltration	LN short diameter, LN volume, Expert rating	- Radiomic model: CT: 0.89 - Competitive model: LN short diameter: 0.76 LN volume: 0.74 Expert rating: 0.65	- Radiomic model: CT: 0.95 - Competitive model: LN short diameter: 0.84 LN volume: 0.80 Expert rating: 0.67	15/36
(Acar et al., 2019)	N = 75, single-centre	Retrospective cohort. Histologically confirmed PCa. All patients underwent previous treatments	- PET/CT - Tracers: ^{68}Ga-PSMA11	- Extracted: 40 features (*histogram, shape, texture)* from sclerotic lesions - Selection method: association with outcome	- Classifier: decision tree, discriminant analysis, support vector machine, K-nearest neighbour, ensemble classifier algorithm - Validation cohort: NO (10-fold cross validation)	Discriminate between metastatic and cured sclerotic lesions	PSMA above liver activity	NA	CT: 0.77	NA	12/36

Summary of the studies investigating the utility of radiomics to detect lymph node infiltration and distant metastases in PCa. GS = Gleason score; NA = Not available; BS = Bone Scintigraphy; BSI = Bone Scan Index; SUV = Standardized Uptake Value; LASSO = least Absolute Shrinkage and Selection Operator. Reported results refer to the classifier that yielded the highest AUC in the study, RQS = Radiomics Quality Score.

Table 7
Radiomics to predict the risk of developing metastases.

Name, year	Data	Clinical setting	Imaging	Radiomic features	Analysis	Outcome	Ground truth	Competitive model	AUC training cohort	AUC validation cohort	RQS
(Cysouw et al., 2020)	N = 76, single-centre	Prospective cohort. Biopsy proven prostate adenocarcinoma. PET scan prior to RP.	- PET - Tracers: [18 F]DCFPyL - MRI	- Extracted: 480 features (*intensity, morphology, texture*) from primary tumour - Selection method: PCA, random forest, univariate ANOVA - Extracted: 976 features *(shape, intensity, intensity histogram, texture*) from primary tumour	- Classifier: Random forest (1000 decision trees) - Validation cohort: NO (5-fold cross validation repeated 50 times) - Classifier: Multivariate regression analysis	Prediction of lymph nodes infiltration	Surgical tissue specimens (prostate and lymph nodes)	Combination of standard PET metrics (SUV_{mean}, SUV_{peak}, SUV_{max}, PSMA-positive tumour volume, PSMA-total lesion uptake)	- Radiomic model: PET: 0.86 - Competitive model: PET: 0.81 - Combined models: NA - Radiomic model:	NA - Radiomic model:	20/36
(Wang et al., 2019)	N = 176, single-centre	Retrospective cohort. Histologically confirmed PCa, without signs of metastasis at diagnosis. Follow-up range: 7–119 months (or until metastasis detected)	- Sequences: T2-w, DCE T1-w	- Selection method: Stepwise, LASSO, and Ridge regression	- Validation cohort: YES (sample split with 3:1 ratio in training (N = 132) and test (N = 44) cohorts)	Prediction of metastases development	Emission computerized tomography	Clinical factors (age, f-PSA level, GS)	T2-w: 0.875 DCE T1-w: 0.875 bp-MRI: 0.898 - Competitive model: GS: 0.731 - Combined models: bp-MRI + clinical factors: 0.916	NA - Competitive model: NA - Combined model: bp-MRI + clinical factors: 0.895	12/36
(Zhang et al., 2020b)	N = 116, single-centre	Retrospective study. PCa newly confirmed by surgery or biopsy. State of the skeleton (presence of metastasis) clearly defined.	- MRI - Sequences: DWI, FST2-w, DCE, T1-w	- Extracted: 204 features from primary tumour - Selection method: LASSO logistic regression	- Classifier: Multivariate stepwise reverse logistic regression - Validation cohort: YES (sample split with 7:3 ratio in training (N = 81) and test (N = 35) cohorts)	Prediction of metastases development	Emission computerized tomography	t-PSA level	- Radiomic model: mp-MRI: 0.86 - Competitive model: t-PSA: 0.85 - Combined models: mp-MRI + t-PSA: 0.93	- Radiomic model: mp-MRI: 0.84 - Competitive model: NA - Combined models: mp-MRI + t-PSA: 0.92	12/36

Summary of the studies investigating the utility of radiomics to predict the risk of developing metastases. RP = Radical prostatectomy; PCA = principal component analysis; f-PSA = free prostate specific antigen, GS = Gleason score; NA = Not Available; RQS = Radiomics quality score.

limitations due, for example, to sampling error.

Several efforts have been recently made to investigate the capacity of radiomics to estimate the clinical significance of PCa. A summary of the studies investigating this topic is provided in Table 3.

The implementation of radiomics to grade PCa almost exclusively relies on retrospective cohorts (23/26 studies), that are often the result of multicentric collaborations (10/26 studies) (Algohary et al., 2020; Woźnicki et al., 2020; Deukwoo et al., 2018; Parra et al., 2018; Brunese et al., 2019, 2020; Chaddad et al., 2020; Zhang et al., 2020a; Chaddad et al., 2018a, b). This setting is facilitated by the presence of challenges that provide free online databases, allowing reproducible and easily comparable analyses that are robust and generalizable.

23 out of 26 studies using radiomics to establish the clinical significance of PCa are based on MRI data (Hou et al., 2020; Algohary et al., 2020; Woźnicki et al., 2020; Deukwoo et al., 2018; Parra et al., 2018; Brunese et al., 2019, 2020; Chaddad et al., 2020; Zhang et al., 2020a; Chaddad et al., 2018a, b; Abdollahi et al., 2019a; Gong et al., 2020; Hectors et al., 2019; Liu et al., 2019; Bonekamp et al., 2018; McGarry et al., 2019; Cuocolo et al., 2019; Bleker et al., 2020; Gugliandolo et al., 2021; Toivonen et al., 2019; yang et al., 2020; Bernatz et al., 2020) two consider computed tomography (CT) (Tanadini-Lang et al., 2018; Osman et al., 2019) and only two researches implemented PET imaging (Zamboglou et al., 2019; Papp et al., 2020). The two classifiers based on CT imaging performed discretely well in the training cohort (AUC up to 0.97) but failed to generalize in external datasets (AUC = 0.65). On the other hand, generalization occurred in one of the PET based study (Zamboglou et al., 2019) (AUC = 0.84 in the validation cohort), making this an interesting approach for future work. The lack of standardization in acquisition protocols that is typical of radiomic analyses does not spare these MRI studies, where the choice of the sequences to be considered remains an open issue. Furthermore, only a few authors (Woźnicki et al., 2020; Zhang et al., 2020a; Gong et al., 2020; yang et al., 2020; Bernatz et al., 2020) combined radiomics with clinical risk factors, creating comprehensive models yielding the highest AUC in a validation cohort (yang et al., 2020) (AUC = 0.91 for the prediction of GS upgrade from biopsy to surgery).

PCa is commonly graded accordingly to GS, however other classifications such as D'Amico risk classification system and Gleason grade (GG) exist. This, although may seem of minor relevance, it involves difficulties for the standardization of studies trying to determine the aggressiveness of PCa with radiomic analysis. Difficulties that are exacerbated by the fact that even within investigations basing their outcomes on the same scale (e.g., GS), different thresholds are considered to be clinically relevant. Some authors (Zamboglou et al., 2019; Abdollahi et al., 2019a; Gong et al., 2020; Hectors et al., 2019; Liu et al., 2019; Tanadini-Lang et al., 2018) regard a GS $\geq$ 8 as clinically significant because at this grade radical interventions represent the best therapy plan for patients, while others (Woźnicki et al., 2020; Deukwoo et al., 2018; Parra et al., 2018; Chaddad et al., 2018a, b; Bleker et al., 2020; Gugliandolo et al., 2021; Toivonen et al., 2019) lower the threshold up to GS $\geq 3 + 4$, arguing that is only a matter of time before the disease will progress further (See Table 3, outcome column). Both are valid approaches with strengths and pitfalls, but the outcome of choice affects the classifier performance because at the microscopic level intermediate grade (GS $\leq$ 7) and high grade (GS $\geq$ 8) PCa look more different than intermediate/low (GS = 3 + 4) compared to intermediate/high (GS = 4 + 3) lesions. This calls for an urgent need of international guidelines for the standardization of the definition of clinical relevance, otherwise, despite the discretely high quality of the research (mean RQS = 11.92), the direct comparison of different approaches, methods, and results will not be feasible.

3.4. Biochemical recurrence prediction

RP and RT are effective treatments for localized PCa. However, about 30 % of patients treated with RP (Freedland et al., 2005) and ~15 % of patients treated with RT (Widmark et al., 2019) experience biochemical recurrence (BCR) of PCa after definitive therapy. BCR, which is usually addressed with early salvage RT, is associated with an increased risk of developing metastases and death from PCa (Freedland et al., 2005). The early identification of subjects at high risk for BCR would allow a better management of the disease, selecting patients that would benefit the most from adjuvant RT and those that could avoid unnecessary complementary treatments and the associated side effects. However, determining who is at risk for BCR is particularly challenging, because all the parameters investigated in clinical practice (e.g., GS, PSA, age) are not associated with BCR (Bourbonne et al., 2019; Dinis Fernandes et al., 2018; Bourbonne et al., 2020).

There is little, but promising, evidence that radiomics has the potential to predict the risk of BCR prior to treatment (Papp et al., 2020; Bourbonne et al., 2019; Dinis Fernandes et al., 2018; Bourbonne et al., 2020; Li et al., 2020b; Shiradkar et al., 2018; Zhong et al., 2020; Bosetti et al., 2020; Gnep et al., 2017). Please, refer to Table 4 for an overview of the works assessing the utility of radiomics for the prediction of BCR.

Seven out of the 9 studies addressing this topic are based on T2-w and ADC extracted RF (Bourbonne et al., 2019; Dinis Fernandes et al., 2018; Bourbonne et al., 2020; Li et al., 2020b; Shiradkar et al., 2018; Zhong et al., 2020; Gnep et al., 2017), in line with the tendency to base radiomic analysis on MR sequences that was seen so far. Conversely to the definition of csPCa, BCR is clearly defined as a PSA increase above 0.2 ng/ml confirmed in two successive blood samples after RP, and by the Phoenix criteria following RT (Roach et al., 2006). Therefore, allowing direct comparisons between different classifiers and methodological pipelines. The limited evidence gathered so far suggests that (i) extracting MRI RF from the prostatic tumour (Bourbonne et al., 2019, 2020; Li et al., 2020b; Shiradkar et al., 2018) or from the whole prostate (Zhong et al., 2020) for the prediction of BCR does not change the classifiers' performance (AUC range in validation set: = 0.71−0.76 and 0.73, respectively); (ii) The predictive ability of radiomics for BCR development is superior to that of clinical factors like GS, pre/post-operative PSA etc., as highlighted by all studies comparing the two modalities (Bourbonne et al., 2019, 2020; Li et al., 2020b), and (iii) Unexpectedly adding clinical variables to radiomics based models hampers their performance in training (Dinis Fernandes et al., 2018) and validation cohorts (Bourbonne et al., 2019, 2020).

Despite the paucity of literature investigating MR based RF for BCR prediction, and the retrospective nature of all these studies, it is worth noting that three works here reported (Bourbonne et al., 2020; Li et al., 2020b; Shiradkar et al., 2018) were multicentric, five (Bourbonne et al., 2019; Li et al., 2020b; Shiradkar et al., 2018) were based on large samples (N > 100) and all of them based their analysis on standardized, clearly defined reference standards, resulting in investigations largely adhering to current guidelines for radiomic analysis as highlighted by the high mean RQS (13.28).

Recently, (Bosetti et al. (2020)) evaluated the utility of cone beam computed tomography (CBCT) RF applied to logistic regression for the prediction of BCR and found extremely encouraging results (AUC = 1). However, the sample was small (N = 30) and affected by class imbalance, with only three cases of BCR at follow-up, making their study, as admitted by the authors themselves, highly susceptible to class imbalance and overfitting issues. Therefore, this result must be interpreted with great caution, and more studies are needed to prove the real benefits from using CBCT radiomics for BCR prediction.

The combination of RF and clinical data resulted in a highly accurate prediction of BCR only in the single study (Papp et al., 2020) using RF extracted from ^{68}Ga-PSMA PET/MRI. Here, a random forest validated with the 1000 folds Monte Carlo cross validation approach was reported to predict BCR with an AUC = 0.90 in a prospectively enrolled cohort. This result is highly encouraging, suggesting that PET based RF could be remarkably informative. However, further studies have to replicate this result to assess the actual utility of ^{68}Ga-PSMA PET/MRI based RF for the prediction of BCR.

Table 8
Radiomics to predict the risk of EPE.

Name, year	Data	Clinical setting	Imaging	Radiomic features	Analysis	Outcome	Ground truth	Competitive model	AUC training cohort	AUC validation cohort	RQS
(Xu et al., 2020)	N = 95, single-centre	Retrospective cohort. Patients with pathologically confirmed PCa. MRI prior to RP	- MRI - Sequences: T2-w, DWI, ADC, DCE	- Extracted: 4580 features (*first order statistic, texture, shape)* from the primary tumour - Selection method: minimum redundancy maximum relevance, LASSO	- Classifier: Logistic regression - Validation cohort: YES (82 lesions used to train the model, 33 to validate it)	Prediction of EPE	Histopathologic assessment	Clinical factors: t-PSA, GG	- Radiomic model: mp-MRI: 0.92 - Competitive model: t-PSA + GG: 0.73 - Combined model: Mp-MRI + clinical factors: 0.92	- Radiomic model: mp-MRI: 0.87 - Competitive model: t-PSA + GG: 0.66 - Combined model: Mp-MRI + clinical factors: 0.86	14/36
(Ma et al., 2019)	N = 210, single-centre	Retrospective cohort. Patients with pathologically confirmed PCa. MRI prior to RP	- MRI - Sequences: T2-w, DWI, DCE	- Extracted: 1619 features *(global, non-texture, texture)* from the prostate boarders - Selection method: Kendall correlation, LASSO	- Classifier: Sigmoidal function - Validation cohort: YES (sample split with 2:1 ratio in training (N = 143) and validation (N = 67) cohorts)	Prediction of EPE	Histopathologic assessment	3 Radiologists' classification	- Radiomic model: mp-MRI: 0.90 - Competitive model: Radiologist 1: 0.69 Radiologist 2: 0.76 Radiologist 3: 0.76	- Radiomic model: mp-MRI: 0.88 - Competitive model: Radiologist 1: 0.60 Radiologist 2: 0.70 Radiologist 3: 0.69	14/36
(Ma et al., 2020)	N = 119, single-centre	Retrospective cohort. Patients with pathologically confirmed PCa. MRI prior to RP	- MRI - Sequences: T2-w, DWI, DCE	- Extracted: 1619 features *(global, non-texture, texture)* from the prostate boarders - Selection method: Kendall correlation, LASSO	- Classifier: Sigmoidal function - Validation cohort: YES (sample split with 3:2 ratio in training (N = 74) and validation (N = 45) cohorts)	Prediction of EPE	Histopathologic assessment	NA	mp-MRI: 0.90	mp-MRI: 0.82	14/36
(Losnegård et al., 2020)	N = 228, single-centre	Retrospective cohort. Patients with pathologically confirmed PCa. MRI prior to RP	- MRI - Sequences: T2-w, ADC, DCE	- Extracted: 254 features *(intensity, texture)* from the whole prostate - Selection method: random forest	- Classifier: Random forest, logistic regression - Validation cohort: NO (10-fold cross validation repeated 100 times)	Prediction of EPE	Histopathologic assessment	MSKCC nomogram, radiologist' classification	- Radiomic model: mp-MRI: 0.75 - Competitive model: MSKCC: 0.67 Radiologist: 0.74 - Combined model: MSKCC + mp-MRI: 0.77 MSKCC + radiologist: 0.77 mp-MRI + radiologist:0.78 MSKCC + radiologist + mp-MRI: 0.80	NA	13/36

Summary of the studies investigating the utility of radiomics to predict extraprostatic extension. EPE = extraprostatic extension; RP = radical prostatectomy; f-PSA = free prostate specific antigen; GG = Gleason grade; MSKCC = Memorial Sloan Kattering Cancer Center; NA = Not Available; RQS = Radiomics Quality Score.

3.5. Radiation therapy outcome prediction and treatment efficacy monitoring

Radiation therapy is a consolidated treatment for PCa, although possible RT induced toxicity should always be taken into account during patient management (Widmark et al., 2019). Selecting those patients that are likely to benefit the most from RT, without experiencing serious adverse effects, is of the utmost importance and represents a necessary step towards precision medicine.

Analysing RF extracted prior to therapy initiation has been shown to be a promising approach to both stratify those patients that will respond to RT (Brunese et al., 2019; Abdollahi et al., 2019a; Wu et al., 2019), and to identify those subjects that are at high risk for radiation induced toxicity (Mostafaei et al., 2020; Rossi et al., 2018; Tsang et al., 2020; Abdollahi et al., 2019b) (Table 5 for a summary of the results). However, although the AUC of studies that use RF extracted from the primary tumour before therapy initiation to predict which patients will be a responder for RT range from 0.7 to more than 0.85, there are still critical issues that need to be addressed before radiomics can be proposed for clinical use. There is not a consensus on which is the main outcome to be considered when deciding whether the treatment was effective or not, nor on the imaging modalities that have to be examined, or the RF that provide the best information. Furthermore, all these studies were monocentric, with sample size < 40, and were not validated in external cohorts.

Rossi et al. in a retrospective evaluation (Rossi et al., 2018) and Mostafaei et al. in a prospective study (Mostafaei et al., 2020) predicted the onset of RT induced adverse effects and showed that including in the analysis RF extracted from rectum and bladder results in better prognostic models compared to those relying on clinical risk factors (non-treatment related parameters combined with dose volume histogram and PSA, prostate volume, dose volume respectively) only. These works suggest that analysing RF extracted from adjacent organs, such as rectum and bladder, provides additional value to standard clinical risk factors, but further studies are needed to confirm these results.

Radiomic analysis, aside from being used to predict treatment outcomes, it can also be implemented to monitor treatment efficacy. Indeed, changes in the set of RF extracted from the tumour site that occur during the therapy period represent quantitative real-time biomarkers for RT effect. Furthermore, changes in RF extracted from adjacent organs, like bladder and rectum, may stem for induced toxicity (Tsang et al., 2020; Lorenz et al., 2019). Both Lee (Lee et al., 2019) and Lorenz (Lorenz et al., 2019) in their investigations reported that 44 and 5 MRI based RF significantly changed after RT, potentially representing quantitative, easy to interpret, biomarkers quickly obtainable in standard practice. However, only two exploratory studies were conducted on this topic so far, and the clinical relevance of the features that were altered by RT has not been cleared yet. The handful of exploratory studies investigating the potential of radiomics to monitor RT efficacy and safety is highly heterogeneous, as remarked by their low mean RQS (6.44). Therefore, an increased effort to improve the standardization of radiomic analysis for this purpose is needed, as much as the presence of future, well-powered, studies to replicate these first interesting findings.

Other issues to be addressed before radiomics can be proposed for clinical practice in the field of RT monitoring are the identification of the subset of robust RF characterizing RT effects, as well as their biological and/or clinical meaning.

3.6. Metastases detection

The presence of distant metastases and lymph nodes (LN) involvement are two of the most relevant prognostic factors in PCa.

Just recently radiomics was proposed to ameliorate lesions detection accuracy, by exploiting all the sub-visual information stored in medical images.

One single retrospective, multicentric study (Peeken et al., 2020) showed that ^{68}Ga-PSMA PET/CT based radiomic analysis could detect histology-confirmed LN infiltrations with AUC = 0.95 in a validation set. Thus, being more accurate than a classification based on the LN short diameter, or on visual inspection only (AUC = 0.84 and 0.67 in a validation cohort, respectively).

Even more scarce is the evidence regarding the ability of radiomics to detect bone metastases. At present, the performance of radiomic analyses for the diagnosis of distant bone metastases have never been compared to that of other instrumental exams. Furthermore, the few studies addressing this topic (Filograna et al., 2019; Acar et al., 2019; Moazemi et al., 2020) are all retrospective, relying on the expert's classification of images to train and test their models and are poorly standardized with a mean RQS = 7.4. Therefore, it is impossible to speculate whether this new approach bears the potential to improve the current clinical standards, outperforming expert physicians.

Artificial intelligence could also be applied for the extraction and analysis of conventional imaging parameters. Wuestemann and colleagues (Wuestemann et al., 2020) implemented an artificial neural network (ANN) to automatically extract bone scan index (BSI) from planar bone scans and reported that a cut-off of 0.27 % was more accurate than the commonly implemented binary division (0 vs > 0) for bone metastasis detection, reaching an AUC = 0.94 and sensitivity and specificity respectively of 87 % and 98 % in a never validated training cohort.

(Acar et al. (2019)) in 2019 provided a proof of principle that radiomics can be utilized to identify metastatic lesions that responded to treatment. Metastatic lesions were defined as sclerotic lesions having PSMA above liver activity. CT texture features were fed to a K-nearest neighbour (KNN) classifier that discriminated metastatic and responded lesions from 75 patients with a PPV = 87 % and NPV = 54 %.

As it can be appreciated from Table 6, where a detailed summary of these studies is provided, all the papers here presented based their results on monocentric studies trained and validated on subjective ground truths. RF are often extracted from avid PET lesions manually identified by expert physicians, thus conclusions regarding the potential of radiomics to overperform human evaluations cannot be drawn.

3.7. Metastases prediction

Preoperatively identifying patients at risk for LN involvement and bone metastasis is crucial for treatment planning. Unfortunately, commonly used clinical nomograms are inadequate for this purpose (Mottet et al., 2020).

Building on the promising results of radiomic analysis for the staging and characterization of PCa, researchers started to explore the utility of radiomics for the prediction of distant metastases development. A summary of the results is provided in Table 7. Both PET (Cysouw et al., 2020), and mp-MRI (Wang et al., 2019; Zhang et al., 2020b) RF extracted from the primary tumour prior to metastases formation have been investigated, either alone (Cysouw et al., 2020) or in combination with clinical risk factors (Wang et al., 2019; Zhang et al., 2020b), creating accurate nomograms (AUC up to ~0.90 in validation cohorts) for the prediction of the risk for distant metastases.

The few studies addressing this topic all compared the performance of their radiomic models with that of clinical factors such as PSA, GS or conventional semi-quantitative PET parameters. Radiomics always provided results at least comparable to that of other classifications in training cohorts (AUC > 0.80), however, the comparisons between classifiers have never been validated in separate sets. On the other hand, a combination of clinical factors and RF has been tested and validated yielding the highest performance for metastases prediction (AUC = 0.92 in a validation cohort (N = 35) combining mp-MRI RF and total PSA) (Zhang et al., 2020b).

The potential utility of radiomic analysis for metastases prediction has just started to be investigated, but evidence gathered so far is promising. Three monocentric works based on samples with N > 75 and

mean RQS = 14.6 paved the way for the study of radiomics based on either PET or mp-MRI. Future studies are needed to assess the utility of radiomics for the preoperative prediction of the development of a metastatic disease.

3.8. Prediction of extra-prostatic extension

The presence of extra-prostatic extension (EPE) in RP is associated with biochemical recurrence and increased risk of death from PCa (Xu et al., 2020). Being able to accurately detect EPE prior to the operation is crucial for treatment planning and potentially improves the prognosis. Clinical factors such as PSA level and GS are associated with the risk of EPE, nomograms have been developed to help clinicians predicting the likelihood of EPE (Kattan et al., 2000), and yet, between 20–30% of EPE cases are currently under-staged in clinical practice (Ma et al., 2020).

Four studies indicate that mp-MRI based radiomics bears the potential to aid radiologists in the preoperative identification of EPE (see Table 8).

RF extracted from the primary tumour (Xu et al., 2020), the prostate boarders (Ma et al., 2020, 2019), and the whole prostate (Losnegård et al., 2020) have been shown to be highly informative for the detection of EPE (AUC ≈ 0.80). Despite the fact that only few studies addressed this topic, there is a clear trend showing how histologically confirmed EPE can be better identified by ML algorithms based on RF rather than by experts looking at MR images or basing their evaluation on clinical factors such as tPSA and Gleason grade. Radiomics was also compared to clinical nomograms normally implemented in standard practice like the Memorial Sloan Kattering Cancer Center (MSKCC). This was done by Losnegard and colleagues (Losnegård et al., 2020) in a retrospective, monocentric study based on 228 patients that has never been validated in a separate dataset. Here, the clinical nomogram was reported to be the worst predictor of EPE, with an AUC of 0.67 in the training cohort, while the performance of the radiomics based classifier and that of the radiologist were comparable (AUC = 0.75). Certainly, further studies are needed to replicate these results, but whenever implemented radiomics based models for the identification of EPE were at least as performing as experienced radiologists in both training and validation cohorts. Another aspect strengthening the findings of these radiomic analyses is that all the studies here reported (i) have N > 90; (ii) the reference standard was always based on the histopathological assessment following RP; (iii) these studies adhere to existing guidelines, mean RQS = 13.75 and (iv) all except for Losnegard et al. were validated in separate cohorts.

4. Discussion

Radiomics bears the potential to aid clinicians for the personalized management of PCa. Radiomic analysis is performed starting from medical images routinely collected in clinical practice and, therefore, is a non-invasive procedure that does not entail additional costs. Furthermore, since it exploits information collected throughout the whole organ it provides notions on tumour heterogeneity. Conversely, biopsy, the state-of-the-art technique to characterize PCa, presents multiple drawbacks including sampling error and patients' discomfort.

Radiomics was first proposed to improve PCa care in 2015, and since then it has been investigated to answer several clinically relevant questions.

Accumulating evidence shows that radiomics may represent a useful tool for PCa screening, even at the early stage of the disease or when images are of difficult interpretation. Furthermore, mp-MRI radiomic analysis have been largely investigated over the last few years as an alternative approach to biopsy for grading PCa, reaching high levels of accuracy (AUC up to ~ 0.9).

Research on the utility of radiomics for the prediction of BCR, treatment monitoring, metastases detection and prediction and EPE prediction is still in its infancy. However, important differences among works addressing different questions emerge already. The little evidence supporting the potential role of radiomics for treatment monitoring often presents ill-defined outcomes, does not rely on solid ground truths, and is based on studies that do not adhere to existing guidelines for optimal research in radiomics. Conversely, the few studies investigating radiomics for BCR, metastases and EPE prediction all rely on large samples, with clear and objective reference standards used to train and validate (often in separate cohorts) their models.

At present, MRI is the most investigated imaging modality in radiomic analysis. However, PET and CT RF were reported to be extremely helpful, especially for the detection and prediction of distant metastases (Peeken et al., 2020; Moazemi et al., 2020; Giesel et al., 2017; Cysouw et al., 2020). Combining features from different imaging modalities will allow a better and more comprehensive characterization of the tumors.

Comparing the performance of RF powered classifiers to that of clinical nomograms commonly used in clinical practice is necessary to establish the additional utility bore by radiomics to the clinical management of PCa and future studies need to incorporate multimodal imaging RF with clinical factors to provide models capable of improving personalized PCa care.

The future of radiomics looks bright, but to date, radiomics is a quickly developing discipline that lacks consolidated methods. More than half of the studies assessing its potential for the clinical management of PCa has not been validated in separate cohorts, and since only thirteen of the studies here reported have been conducted with a multicenter setting, practically none of the results has been validated in external, independent samples. Datasets are often small, and variables within them are frequently unbalanced, resulting in increased probability of over-fitting. Since MRI is highly over-represented in radiomic analysis as compared to PET, CT or US, it is not clear yet which imaging modality stores the highest amount of information for a specific task, nor how to efficiently combine multiple imaging modalities in comprehensive models.

While the clinical problem that several researchers address is clear, the operationalization of the investigated outcomes is sometimes vague and often too heterogeneous, making it difficult to directly compare results. Comparison that is further hampered by the implementation of different ML/DL classifiers that influence the results.

There is an evident endeavor to standardize and improve the robustness of radiomic analyses that resulted in the implementation of guidelines such as the RQS. This consists in a checklist evaluating all the steps of a general radiomic analysis, ranging from data selection to statistical modeling going through the features' selection and extraction processes. The ideal investigation in radiomics according to the RQS would collect 36 points. However, this is an extremely helpful tool that provides useful information regarding the quality and potential reproducibility of a radiomic study but is far from perfect. Discussing the limitations of the RQS is not the purpose of this review, and the importance of the presence of checklists to guide research in radiomics cannot be stressed too much. Noting that RQS is strongly affected by the investigated topic (sometimes objective ground truths are difficult, if possible, to obtain) and does not fit well in DL based radiomics, anyway, is necessary to understand the low score of some well-designed investigations.

5. Conclusion

In conclusion, this work systematically reviewed all the applications of radiomic analysis for the clinical management of PCa, showing the great potential that it bears and the many limitations that still prevent it to enter clinical practice. Results gathered so far are encouraging, but often exploratory and non-comparable. Future studies with larger samples and external validation cohorts, including multimodal imaging RF and clinical factors are needed to assess with certainty the utility of radiomic analysis for the improvement of PCa care.

Ethical approval and consent to participate

Not applicable.

Consent for publication

Not applicable.

Declaration of Competing Interest

All the Authors have no conflicts of interest to disclose related to the present paper.

Acknowledgements

This work was supported by the Italian Association for Cancer Research (grant IG 2017 Id. 20571) and by the Italian Ministry of Health (PE-2016-02361273); EUDRACT number: 2018-001034-18.

References

Abdollahi, H., Mofid, B., Shiri, I., Razzaghdoust, A., Saadipoor, A., Mahdavi, A., et al., 2019a. Machine learning-based radiomic models to predict intensity-modulated radiation therapy response, Gleason score and stage in prostate cancer. Radiol Medica.

Abdollahi, H., Tanha, K., Mofid, B., Razzaghdoust, A., Saadipoor, A., Khalafi, L., et al., 2019b. MRI radiomic analysis of IMRT-Induced bladder wall changes in prostate Cancer patients: a relationship with radiation dose and toxicity. J. Med. Imaging Radiat. Sci.

Acar, E., Leblebici, A., Ellidokuz, B.E., Başbinar, Y., Kaya, G.Ç., 2019. Machine learning for differentiating metastatic and completely responded sclerotic bone lesion in prostate cancer: a retrospective radiomics study. Br. J. Radiol.

Algohary, A., Viswanath, S., Shiradkar, R., Ghose, S., Pahwa, S., Moses, D., et al., 2018. Radiomic features on MRI enable risk categorization of prostate cancer patients on active surveillance: preliminary findings. J. Magn. Reson. Imaging.

Algohary, A., Shiradkar, R., Pahwa, S., Purysko, A., Verma, S., Moses, D., et al., 2020. Combination of peri-tumoral and intra-tumoral radiomic features on bi-parametric mri accurately stratifies prostate cancer risk: A multi-site study. Cancers (Basel).

American College of Radiology Web site, 2015. PI-RADS Prostate Imaging and Reporting and Data System: Version 2 [Internet]. Available from: http://www.acr.org/~/media/ACR/Documents/PDF/QualitySafety/Resources/PIRADS/PIRADS V2.pdf.

Andor, N., Graham, T.A., Jansen, M., Xia, L.C., Aktipis, C.A., Petritsch, C., et al., 2016. Pan-cancer analysis of the extent and consequences of intratumor heterogeneity. Nat. Med.

Bagher-Ebadian, H., Janic, B., Liu, C., Pantelic, M., Hearshen, D., Elshaikh, M., et al., 2019. Detection of dominant intra-prostatic lesions in patients with prostate Cancer Using an artificial neural network and MR multi-modal radiomics analysis. Front. Oncol.

Bernatz, S., Ackermann, J., Mandel, P., Kaltenbach, B., Zhdanovich, Y., Harter, P.N., et al., 2020. Comparison of machine learning algorithms to predict clinically significant prostate cancer of the peripheral zone with multiparametric MRI using clinical assessment categories and radiomic features. Eur. Radiol.

Bleker, J., Kwee, T.C., Dierckx, R.A.J.O., de Jong, I.J., Huisman, H., Yakar, D., 2020. Multiparametric MRI and auto-fixed volume of interest-based radiomics signature for clinically significant peripheral zone prostate cancer. Eur. Radiol.

Bonekamp, D., Kohl, S., Wiesenfarth, M., Schelb, P., Radtke, J.P., Götz, M., et al., 2018. Radiomic machine learning for characterization of prostate lesions with MRI: comparison to ADC values. Radiology.

Bosetti, D.G., Ruinelli, L., Piliero, M.A., van der Gaag, L.C., Pesce, G.A., Valli, M., et al., 2020. Cone-beam computed tomography-based radiomics in prostate cancer: a mono-institutional study. Strahlenther. Onkol.

Bourbonne, V., Vallières, M., Lucia, F., Doucet, L., Visvikis, D., Tissot, V., et al., 2019. MRI-derived radiomics to guide post-operative management for high-risk prostate cancer. Front. Oncol.

Bourbonne, V., Fournier, G., Vallières, M., Lucia, F., Doucet, L., Tissot, V., et al., 2020. External validation of an MRI-derived radiomics model to predict biochemical recurrence after surgery for high-risk prostate cancer. Cancers (Basel).

Brunese, L., Mercaldo, F., Reginelli, A., Santone, A., 2019. Prostate gleason score detection and cancer treatment through real-time formal verification. IEEE Access.

Brunese, L., Mercaldo, F., Reginelli, A., Santone, A., 2020. Radiomics for gleason score detection through deep learning. Sensors (Switzerland).

Cameron, A., Khalvati, F., Haider, M.A., Wong, A., 2016. MAPS: A Quantitative Radiomics Approach for Prostate Cancer Detection. IEEE Trans. Biomed. Eng.

Carlaw, K.R., Woo, H.H., 2017. Evaluation of the changing landscape of prostate cancer diagnosis and management from 2005 to 2016. Prostate Int.

Chaddad, A., Niazi, T., Probst, S., Bladou, F., Anidjar, M., Bahoric, B., 2018a. Predicting gleason score of prostate cancer patients using radiomic analysis. Front. Oncol.

Chaddad, A., Kucharczyk, M.J., Niazi, T., 2018b. Multimodal radiomic features for the predicting gleason score of prostate cancer. Cancers (Basel).

Chaddad, A., Kucharczyk, M.J., Desrosiers, C., Okuwobi, I.P., Katib, Y., Zhang, M., et al., 2020. Deep radiomic analysis to predict gleason score in prostate Cancer. IEEE Access.

Chen, T., Li, M., Gu, Y., Zhang, Y., Yang, S., Wei, C., et al., 2019. Prostate Cancer differentiation and aggressiveness: assessment with a radiomic-based model vs. PI-RADS v2. J. Magn. Reson. Imaging.

Chung, A.G., Khalvati, F., Shafiee, M.J., Haider, M.A., Wong, A., 2015. Prostate cancer detection via a quantitative radiomics-driven conditional random field framework. IEEE Access.

Cuocolo, R., Stanzione, A., Ponsiglione, A., Romeo, V., Verde, F., Creta, M., et al., 2019. Clinically significant prostate cancer detection on MRI: a radiomic shape features study. Eur. J. Radiol.

Cysouw, M.C.F., Jansen, B.H.E., van de Brug, T., Oprea-Lager, D.E., Pfaehler, E., de Vries, B.M., et al., 2020. Machine learning-based analysis of [18F]DCFPyL PET radiomics for risk stratification in primary prostate cancer. Eur J Nucl Med Mol Imaging. European Journal of Nuclear Medicine and Molecular Imaging 48, 340–349.

Deukwoo, K., Reis, I., Breto, A., Zavala-Romero, O., Ford, J., Pollack, A., 2018. Classification of suspicious lesions on prostate multiparametric MRI using machine learning. J. Med. Imaging Bellingham (Bellingham).

Dinis Fernandes, C., Dinh, C.V., Walraven, I., Heijmink, S.W., Smolic, M., van Griethuysen, J.J.M., et al., 2018. Biochemical recurrence prediction after radiotherapy for prostate cancer with T2w magnetic resonance imaging radiomic features. Phys Imaging Radiat Oncol.

Domachevsky, L., Goldberg, N., Bernstine, H., Nidam, M., Groshar, D., 2018. Quantitative characterisation of clinically significant intra-prostatic cancer by prostate-specific membrane antigen (PSMA) expression and cell density on PSMA-11. Eur. Radiol.

Dulhanty, C., Wang, L., Cheng, M., Gunraj, H., Khalvati, F., Haider, M.A., et al., 2020. Radiomics driven diffusion weighted imaging sensing strategies for zone-level prostate cancer sensing. Sensors (Switzerland).

European Association of Urology, 2020. EAU Guidelines [Internet]. Available from: http://uroweb.org/guidelines/compilations-of-all-guidelines/.

Filograna, L., Lenkowicz, J., Cellini, F., Dinapoli, N., Manfrida, S., Magarelli, N., et al., 2019. Identification of the most significant magnetic resonance imaging (MRI) radiomic features in oncological patients with vertebral bone marrow metastatic disease: a feasibility study. Radiol Medica.

Freedland, S.J., Humphreys, E.B., Mangold, L.A., Eisenberger, M., Dorey, F.J., Walsh, P. C., et al., 2005. Risk of prostate cancer-specific mortality following biochemical recurrence after radical prostatectomy. J. Am. Med. Assoc.

Gholizadeh, N., Simpson, J., Ramadan, S., Denham, J., Lau, P., Siddique, S., et al., 2020. Voxel-based supervised machine learning of peripheral zone prostate cancer using noncontrast multiparametric MRI. J. Appl. Clin. Med. Phys.

Giambelluca, D., Cannella, R., Vernuccio, F., Comelli, A., Pavone, A., Salvaggio, L., et al., 2021. PI-RADS 3 lesions: role of prostate MRI texture analysis in the identification of prostate Cancer. Curr. Probl. Diagn. Radiol.

Giesel, F.L., Schneider, F., Kratochwil, C., Rath, D., Moltz, J., Holland-Letz, T., et al., 2017. Correlation between SUVmax and CT radiomic analysis using lymph node density in PET/CT-based lymph node staging. J. Nucl. Med. 58, 282–287.

Gillies, R.J., Kinahan, P.E., Hricak, H., 2016. Radiomics: Images are more than pictures, they are data. Radiology.

Ginsburg, S.B., Algohary, A., Pahwa, S., Gulani, V., Ponsky, L., Aronen, H.J., et al., 2017. Radiomic features for prostate cancer detection on MRI differ between the transition and peripheral zones: preliminary findings from a multi-institutional study. J. Magn. Reson. Imaging.

Gnep, K., Fargeas, A., Gutiérrez-Carvajal, R.E., Commandeur, F., Mathieu, R., Ospina, J. D., et al., 2017. Haralick textural features on T2-weighted MRI are associated with biochemical recurrence following radiotherapy for peripheral zone prostate cancer. J. Magn. Reson. Imaging.

Gong, L., Xu, M., Fang, M., Zou, J., Yang, S., Yu, X., et al., 2020. Noninvasive prediction of high-grade prostate Cancer via biparametric MRI radiomics. J. Magn. Reson. Imaging.

Gugliandolo, S.G., Pepa, M., Isaksson, L.J., Marvaso, G., Raimondi, S., Botta, F., et al., 2021. MRI-based radiomics signature for localized prostate cancer: a new clinical tool for cancer aggressiveness prediction? Sub-study of prospective phase II trial on ultra-hypofractionated radiotherapy (AIRC IG-13218). Eur. Radiol.

Guo, T., Li, L., Zhong, Q., Rupp, N.J., Charmpi, K., Wong, C.E., et al., 2018. Multi-region proteome analysis quantifies spatial heterogeneity of prostate tissue biomarkers. Life Sci Alliance.

Gupta, R.T., Kauffman, C.R., Polascik, T.J., Taneja, S.S., Rosenkrantz, A.B., 2013. The state of prostate MRI in 2013. Oncol (United States).

Hansen, N.L., Koo, B.C., Warren, A.Y., Kastner, C., Barrett, T., 2017. Sub-differentiating equivocal PI-RADS-3 lesions in multiparametric magnetic resonance imaging of the prostate to improve cancer detection. Eur. J. Radiol.

Hectors, S.J., Cherny, M., Yadav, K.K., Beksaç, A.T., Thulasidass, H., Lewis, S., et al., 2019. Radiomics features measured with multiparametric magnetic resonance imaging predict prostate cancer aggressiveness. J. Urol.

Herrmann, K., Veit-Haibach, P., Weber, W.A., 2019. Driving the future of nuclear medicine. J. Nucl. Med.

Hou, Y., Bao, M.L., Wu, C.J., Zhang, J., Zhang, Y.D., Bin, Shi H., 2020. A radiomics machine learning-based redefining score robustly identifies clinically significant prostate cancer in equivocal PI-RADS score 3 lesions. Abdom. Radiol. (NY).

Jordan, E.J., Fiske, C., Zagoria, R.J., Westphalen, A.C., 2017. Evaluating the performance of PI-RADS v2 in the non-academic setting. Abdom. Radiol. (NY).

Kasel-Seibert, M., Lehmann, T., Aschenbach, R., Guettler, F.V., Abubrig, M., Grimm, M. O., et al., 2016. Assessment of PI-RADS v2 for the detection of prostate Cancer. Eur. J. Radiol.

Kattan, M.W., Zelefsky, M.J., Kupelian, P.A., Scardino, P.T., Fuks, Z., Leibel, S.A., 2000. Pretreament nomogram for predicting the outcome of three-dimensional conformal radiotherapy in prostate cancer. J. Clin. Oncol.

Khalvati, F., Wong, A., Haider, M.A., 2015. Automated prostate cancer detection via comprehensive multi-parametric magnetic resonance imaging texture feature models. BMC Med. Imaging.

Khalvati, F., Zhang, J., Chung, A.G., Shafiee, M.J., Wong, A., Haider, M.A., 2018. MPCaD: a multi-scale radiomics-driven framework for automated prostate cancer localization and detection. BMC Med. Imaging.

Kristiansen, G., 2012. Diagnostic and prognostic molecular biomarkers for prostate cancer. Histopathology.

Lambin, P., Leijenaar, R.T.H., Deist, T.M., Peerlings, J., de Jong, E.E.C., van Timmeren, J., et al., 2017. Radiomics: the bridge between medical imaging and personalized medicine. Nat Rev Clin Oncol [Internet] 14, 749–762. Available from: http://www.nature.com/articles/nrclinonc.2017.141.

Lee, S.L., Lee, J., Craig, T., Berlin, A., Chung, P., Ménard, C., et al., 2019. Changes in apparent diffusion coefficient radiomics features during dose-painted radiotherapy and high dose rate brachytherapy for prostate cancer. Phys Imaging Radiat Oncol.

Li, M., Chen, T., Zhao, W., Wei, C., Li, X., Duan, S., et al., 2020a. Radiomics prediction model for the improved diagnosis of clinically significant prostate cancer on biparametric MRI. Quant. Imaging Med. Surg.

Li, L., Shiradkar, R., Leo, P., Algohary, A., Fu, P., Tirumani, S.H., et al., 2020b. A novel imaging based Nomogram for predicting post-surgical biochemical recurrence and adverse pathology of prostate cancer from pre-operative bi-parametric MRI. EBioMedicine.

Liu, B., Cheng, J., Guo, D.J., He, X.J., Luo, Y.D., Zeng, Y., et al., 2019. Prediction of prostate cancer aggressiveness with a combination of radiomics and machine learning-based analysis of dynamic contrast-enhanced MRI. Clin. Radiol.

Lorenz, J.W., Schott, D., Rein, L., Mostafaei, F., Noid, G., Lawton, C., et al., 2019. Serial T2-Weighted magnetic resonance images acquired on a 1.5 tesla magnetic resonance linear accelerator reveal radiomic feature variation in organs at risk: an exploratory analysis of novel metrics of tissue response in prostate Cancer. Cureus.

Losnegård, A., Reisæter, L.A.R., Halvorsen, O.J., Jurek, J., Assmus, J., Arnes, J.B., et al., 2020. Magnetic resonance radiomics for prediction of extraprostatic extension in non-favorable intermediate- and high-risk prostate cancer patients. Acta radiol.

Ma, S., Xie, H., Wang, H., Han, C., Yang, J., Lin, Z., et al., 2019. MRI-Based Radiomics Signature for the Preoperative Prediction of Extracapsular Extension of Prostate Cancer. J. Magn. Reson. Imaging.

Ma, S., Xie, H., Wang, H., Yang, J., Han, C., Wang, X., et al., 2020. Preoperative prediction of extracapsular extension: radiomics signature based on magnetic resonance imaging to stage prostate Cancer. Mol. Imaging Biol.

Marusyk, A., Polyak, K., 2010. Tumor heterogeneity: causes and consequences. Biochim. Biophys. Acta - Rev. Cancer.

McGarry, S.D., Bukowy, J.D., Iczkowski, K.A., Unteriner, J.G., Duvnjak, P., Lowman, A. K., et al., 2019. Gleason probability maps: a radiomics tool for mapping prostate Cancer likelihood in MRI space. Tomogr (Ann Arbor, Mich).

Moazemi, S., Khurshid, Z., Erle, A., Lütje, S., Essler, M., Schultz, T., et al., 2020. Machine learning facilitates hotspot classification in PSMA-PET/CT with nuclear medicine specialist accuracy. Diagnostics. 10.

Monti, S., Brancato, V., Di Costanzo, G., Basso, L., Puglia, M., Ragozzino, A., et al., 2020. Multiparametric MRI for prostate cancer detection: new insights into the combined use of a radiomic approach with advanced acquisition protocol. Cancers (Basel).

Mostafaei, S., Abdollahi, H., Kazempour Dehkordi, S., Shiri, I., Razzaghdoust, A., Zoljalali Moghaddam, S.H., et al., 2020. CT imaging markers to improve radiation toxicity prediction in prostate cancer radiotherapy by stacking regression algorithm. Radiol Medica.

Mottet, N., Bastian, P., Bellmunt, J., van den Bergh, R., Bolla, M., van Casteren, N., et al., 2020. EAU - EANM - ESTRO - ESUR - SIOG: guidelines on prostate Cancer. Eur Assoc Urol.

Orczyk, C., Villers, A., Rusinek, H., Lepennec, V., Bazille, C., Giganti, F., et al., 2019. Prostate cancer heterogeneity: texture analysis score based on multiple magnetic resonance imaging sequences for detection, stratification and selection of lesions at time of biopsy. BJU Int.

Osman, S.O.S., Leijenaar, R.T.H., Cole, A.J., Lyons, C.A., Hounsell, A.R., Prise, K.M., et al., 2019. Computed tomography-based radiomics for risk stratification in prostate Cancer. Int. J. Radiat. Oncol. Biol. Phys.

Papp, L., Spielvogel, C.P., Grubmüller, B., Grahovac, M., Krajnc, D., Ecsedi, B., et al., 2020. Supervised machine learning enables non-invasive lesion characterization in primary prostate cancer with [68Ga]Ga-PSMA-11 PET/MRI. Eur J Nucl Med Mol Imaging. European Journal of Nuclear Medicine and Molecular Imaging.

Parra, N.A., Lu, H., Li, Q., Stoyanova, R., Pollack, A., Punnen, S., et al., 2018. Predicting clinically significant prostate cancer using DCE-MRI habitat descriptors. Oncotarget.

Patel, A.P., Tirosh, I., Trombetta, J.J., Shalek, A.K., Gillespie, S.M., Wakimoto, H., et al., 2014. Single-cell RNA-seq highlights intratumoral heterogeneity in primary glioblastoma. Science (80-).

Peeken, J.C., Shouman, M.A., Kroenke, M., Rauscher, I., Maurer, T., Gschwend, J.E., et al., 2020. A CT-based radiomics model to detect prostate cancer lymph node metastases in PSMA radioguided surgery patients. Eur. J. Nucl. Med. Mol. Imaging.

Qi, Y., Zhang, S., Wei, J., Zhang, G., Lei, J., Yan, W., et al., 2020. Multiparametric MRI-Based Radiomics for Prostate Cancer Screening With PSA in 4–10 ng/mL to Reduce Unnecessary Biopsies. J. Magn. Reson. Imaging.

Roach, M., Hanks, G., Thames, H., Schellhammer, P., Shipley, W.U., Sokol, G.H., et al., 2006. Defining biochemical failure following radiotherapy with or without hormonal therapy in men with clinically localized prostate cancer: recommendations of the RTOG-ASTRO Phoenix consensus Conference. Int J Radiat Oncol [Internet]. 65, 965–974. Available from: https://linkinghub.elsevier.com/retrieve/pii/S0360301606006638.

Rosenkrantz, A.B., Ginocchio, L.A., Cornfeld, D., Froemming, A.T., Gupta, R.T., Turkbey, B., et al., 2016. Interobserver reproducibility of the PI-RADS version 2 lexicon: a multicenter study of six experienced prostate radiologists. Radiology.

Rossi, L., Bijman, R., Schillemans, W., Aluwini, S., Cavedon, C., Witte, M., et al., 2018. Texture analysis of 3D dose distributions for predictive modelling of toxicity rates in radiotherapy. Radiother. Oncol.

Schröder, F.H., Hugosson, J., Roobol, M.J., Tammela, T.L.J., Ciatto, S., Nelen, V., et al., 2009. Screening and prostate-cancer mortality in a randomized european study. N. Engl. J. Med.

Shiradkar, R., Podder, T.K., Algohary, A., Viswanath, S., Ellis, R.J., Madabhushi, A., 2016. Radiomics based targeted radiotherapy planning (Rad-TRaP): a computational framework for prostate cancer treatment planning with MRI. Radiat Oncol [Internet]. Radiation Oncology 11, 1–14. https://doi.org/10.1186/s13014-016-0718-3. Available from:

Shiradkar, R., Ghose, S., Jambor, I., Taimen, P., Ettala, O., Purysko, A.S., et al., 2018. Radiomic features from pretreatment biparametric MRI predict prostate cancer biochemical recurrence: Preliminary findings. J. Magn. Reson. Imaging.

Tanadini-Lang, S., Bogowicz, M., Veit-Haibach, P., Huellner, M., Pauli, C., Shukla, V., et al., 2018. Exploratory radiomics in computed tomography perfusion of prostate cancer. Anticancer Res.

Toivonen, J., Perez, I.M., Movahedi, P., Merisaari, H., Pesola, M., Taimen, P., et al., 2019. Radiomics and machine learning of multisequence multiparametric prostate MRI: towards improved non-invasive prostate cancer characterization. PLoS One.

Tsang, Y.M., Vignarajah, D., McWilliam, A., Tharmalingam, H., Lowe, G., Choudhury, A., et al., 2020. A pilot study on dosimetric and radiomics analysis of urethral strictures following HDR brachytherapy as monotherapy for localized prostate cancer. Br. J. Radiol.

Wang, J., Wu, C.J., Bao, M.L., Zhang, J., Wang, X.N., Zhang, Y.D., 2017. Machine learning-based analysis of MR radiomics can help to improve the diagnostic performance of PI-RADS v2 in clinically relevant prostate cancer. Eur. Radiol.

Wang, Y., Yu, B., Zhong, F., Guo, Q., Li, K., Hou, Y., et al., 2019. MRI-based texture analysis of the primary tumor for pre-treatment prediction of bone metastases in prostate cancer. Magn. Reson. Imaging.

Widmark, A., Gunnlaugsson, A., Beckman, L., Thellenberg-Karlsson, C., Hoyer, M., Lagerlund, M., et al., 2019. Ultra-hypofractionated versus conventionally fractionated radiotherapy for prostate cancer: 5-year outcomes of the HYPO-RT-PC randomised, non-inferiority, phase 3 trial. . Lancet [Internet]. 394, 385–395. Available from: https://linkinghub.elsevier.com/retrieve/pii/S0140673619311316.

Wildeboer, R.R., Mannaerts, C.K., van Sloun, R.J.G., Budäus, L., Tilki, D., Wijkstra, H., et al., 2020. Automated multiparametric localization of prostate cancer based on B-mode, shear-wave elastography, and contrast-enhanced ultrasound radiomics. Eur. Radiol.

World Health Organization, 2020. Cancer Today [Internet]. Available from: https://gco.iarc.fr/today/online-analysis-multi-bars?v=2020&mode=cancer&mode_population=countries&population=900&populations=900&key=total&sex=1&cancer=39&type=0&statistic=5&prevalence=0&population_group=0&ages_group%5B%5D=0&ages_group%5B%5D=17&nb_items=1.

Woźnicki, P., Westhoff, N., Huber, T., Riffel, P., Froelich, M.F., Gresser, E., et al., 2020. Multiparametric MRI for prostate cancer characterization: combined use of radiomics model with PI-RADS and clinical parameters. Cancers (Basel).

Wu, S., Jiao, Y., Zhang, Y., Ren, X., Li, P., Yu, Q., et al., 2019. Imaging-based individualized response prediction of carbon ion radiotherapy for prostate cancer patients. Cancer Manag. Res.

Wuestemann, J., Hupfeld, S., Kupitz, D., Genseke, P., Schenke, S., Pech, M., et al., 2020. Analysis of bone scans in various tumor entities using a deep-learning-based artificial neural network algorithm—evaluation of diagnostic performance. Cancers (Basel).

Xu, M., Fang, M., Zou, J., Yang, S., Yu, D., Zhong, L., et al., 2019. Using biparametric MRI radiomics signature to differentiate between benign and malignant prostate lesions. Eur. J. Radiol.

Xu, L., Zhang, G., Zhao, L., Mao, L., Li, X., Yan, W., et al., 2020. Radiomics based on multiparametric magnetic resonance imaging to predict extraprostatic extension of prostate Cancer. Front. Oncol.

yang, Zhang Gmu, qi, Han Y., wei, Wei J., fei, Qi Y., D sheng, Gu, Lei, J., et al., 2020. Radiomics based on MRI as a biomarker to guide therapy by predicting upgrading of prostate Cancer From biopsy to radical prostatectomy. J. Magn. Reson. Imaging.

Yip, S.S.F., Aerts, H.J.W.L., 2016. Applications and limitations of radiomics. Phys. Med. Biol.

Zamboglou, C., Carles, M., Fechter, T., Kiefer, S., Reichel, K., Fassbender, T.F., et al., 2019. Radiomic features from PSMA PET for non-invasive intraprostatic tumor discrimination and characterization in patients with intermediate- and high-risk prostate cancer – a comparison study with histology reference. Theranostics.

Zamboglou, C., Bettermann, A.S., Gratzke, C., Mix, M., Ruf, J., Kiefer, S., et al., 2020. Uncovering the invisible—prevalence, characteristics, and radiomics feature–based detection of visually undetectable intraprostatic tumor lesions in 68GaPSMA-11 PET images of patients with primary prostate cancer. Eur. J. Nucl. Med. Mol. Imaging.

Zhang, Y., Chen, W., Yue, X., Shen, J., Gao, C., Pang, P., et al., 2020a. Development of a novel, multi-parametric, MRI-Based radiomic nomogram for differentiating between clinically significant and insignificant prostate Cancer. Front. Oncol.
Zhang, W., Mao, N., Wang, Y., Xie, H., Duan, S., Zhang, X., et al., 2020b. A Radiomics nomogram for predicting bone metastasis in newly diagnosed prostate cancer patients. Eur. J. Radiol.
Zhong, Q.Z., Long, L.H., Liu, A., Li, C.M., Xiu, X., Hou, X.Y., et al., 2020. Radiomics of multiparametric MRI to predict biochemical recurrence of localized prostate Cancer After radiation therapy. Front. Oncol.

Samuele Ghezzo, MSc.: Ph.D. student in Molecular Medicine at Vita-Salute San Raffaele University. His main interest is the application of machine/deep learning algorithms to medical imaging for improved clinical management of oncological diseases.

Carolina Bezzi, MSc.: Research fellow at the Nuclear Medicine Department of IRCCS San Raffaele Scientific Institute. Her activities are related to bioinformatics and data science, and her main interests are focused on radiomics and the generation of artificial intelligence-based clinical decision support technologies.

Luca Presotto, Ph.D.: Physicist and certified medical physics expert. He is a Research fellow at the Nuclear Medicine Department of IRCCS San Raffaele Scientific Institute. His research interests involve image processing and artificial intelligence.

Paola Mapelli, M.D., Ph.D.: Nuclear Medicine Physician at the Nuclear Medicine Department of IRCCS San Raffaele Scientific Institute and research fellow at Vita-Salute San Raffaele University. Her main research interests include the use of hybrid Molecular Imaging (PET/CT and PET/MRI) in oncology.

Valentino Bettinardi, MSc: Senior Physicist, staff of the Nuclear Medicine Department of IRCCS San Raffaele Scientific Institute. His research interests include use and development of Positron Emission Tomography (PET), Computed Tomography (CT), Magnetic Resonance Imaging (MRI), hybrid PET/CT and PET/MRI systems. Image processing, Image & data analysis, and PET Image reconstruction (2D and 3D)

Annarita Savi, MSc.: Physicist and certified medical physics expert, staff of the Nuclear Medicine Department of IRCCS San Raffaele Scientific Institute. Her activities are related to therapeutic and diagnostic applications of radionuclides, image analysis and dose patient monitoring.

Ilaria Neri, Biomedical engineer, MSc.: Research fellow at the Nuclear Medicine Department of IRCCS San Raffaele Scientific Institute. Her research activities are related to hybrid PET/MR image processing.

Erik Preza, M.D.: Nuclear Medicine physician at the Nuclear Medicine Department of IRCCS San Raffaele Scientific Institute. His main research interests are related to prostate cancer PET/CT and PET/MRI studies.

Ana Maria Samanes Gajate, M.D.: Nuclear Medicine physician at the Nuclear Medicine Department of IRCCS San Raffaele Scientific Institute, with more than 10 years of experience in the field of Nuclear Medicine. Main research interests include the use of hybrid Molecular Imaging (PET/CT and PET/MRI) in oncology, with special focus on genitourinary cancers.

Francesco De Cobelli, M.D.: Full professor of Radiology at Vita-Salute San Raffaele University; head physician of Clinical and Experimental Radiology Unit, IRCCS San Raffaele Scientific Institute. Director, Postgraduate School of Radiology and director of the PhD course in Molecular Medicine at Vita-Salute San Raffaele University. Responsible for the Experimental and Clinical Radiology Unit of the Experimental Imaging Centre, IRCCS San Raffaele Scientific Institute.

Paola Scifo, Electronic Engineer, PhD.: Senior researcher at the Nuclear Medicine Department at IRCCS San Raffaele Scientific Institute, expert in MR technology, advanced MR applications and image processing. Her actual interests are focused on PET/MRI.

Maria Picchio, M.D.: Associate Professor of Nuclear Medicine at Vita-Salute San Raffaele University; Head of Molecular imaging Unit, Clinical Research Unit of the Experimental Imaging Centre, IRCCS San Raffaele Scientific Institute; Nuclear Medicine physician at the Nuclear Medicine Department of IRCCS San Raffaele Scientific Institute.